A Comparison of Continuous Clocking 1x3 Mode to Timed Exposure Mode Efficiencies of ACIS

S. C. Taylor, N. S. Schulz, H. L. Marshall, D. Dewey

Center for Space Research, M.I.T., Cambridge, MA 02139

September 1999

ABSTRACT

In this document we compare event detection efficiencies in the TE mode to the ones expected in the CC(1x3) mode in the ACIS-S detector array of the HETG spectrometer on board the Chandra X-ray Observatory. Data taken in TE mode have pulse heights determined from the charge in a 3x3 pixel event island. In CC(1x3) mode, events are read out on a row by row basis, and therefore the pulse height for an event is determined instead from a 1x3 pixel event island. While the QE of ACIS in TE mode has been well characterized, that of CC(1x3) mode remained quite unknown. Therefore, we investigate the changes in QE when using the CC(1x3) mode compared to the TE mode. We used data taken at XRCF in TE mode, and split each 3x3 event island into three 1x3 event islands.The main goal of the analysis is to develop guidelines for a proper order extraction for HETG CC(1x3) mode data.

Our analysis shows a 5% drop in QE in CC(1x3) mode at the O Kα line at 525 eV for FI devices, and a 20% drop for the BI devices. The maximum drop in QE depends on the size of the extraction bandwidth and is 55% around 3 keV for BI and around 50% at 8 keV for FI devices. The number of additional events created during the 3x3 to 1x3 island transformation can be up to 35% throughout the entire energy band. However, when the match of CC(1x3) mode QE is relaxed to 95% of the TE mode QE, the amount of contamination from additional events is greatly reduced.

1. INTRODUCTION

For a detailed introduction of the AXAF CCD Imaging Spectrometer (ACIS) we refer to document SOP-1 (The Science Instrument Operations Handbook) and the ACIS IPI Team Calibration report.[2,5] In this report we focus on data from the ACIS-Spectrometer array (ACIS-S), which is in the focal plane of the High Energy Transmission Grating Spectrometer (HETGS). Readout modes for ACIS include the Timed Exposure (TE) and the Continuous Clocking (CC) mode. In TE mode a full frame consisting of 256 pixel columns and 1024 pixel rows is read out with times that can be chosen between 0.2 and 10.0 seconds. The standard readout time is 3.3 seconds, which is the smallest full frame time with minimum dead time loss.

Event detection in TE mode is based on a 3x3 pixel island grading algorithm (or 5x5 event islands for fainter sources). Currently for calibration purposes we use the standard ASCA grading scheme; some more refined schemes may be used at a later time. The standard grade set we use throughout this analysis is the combined ASCA grades 0,2,3,4, and 6, in which an event threshold is set to 38 for front-illuminated (FI) devices and 20 for back-illuminated (BI) devices, as well as a split threshold of 13 for all devices. The quantum efficiencies (QE) of all devices are calibrated to this standard. For a more detailed description of the implementation of ACIS event grading schemes we refer to the latest documentations.[3,4]

In CC mode, each of the 1024 pixel rows is read out separately, each of which takes about 3 milliseconds. Event detection is now restricted to 1x3 pixel islands, severely limiting the degrees of freedom to recognize an event. Although an option for the creation of data in CC(3x3) mode (by reassembling the 1x3 events back into 3x3 events) is now available, this option is not the standard configuration, and there are other limitations associated with it. Therefore, a thorough investigation into 1x3 mode is necessary. *From here on in this report, we will refer only to CC(1x3) mode data.*

Figure 1 shows an example of the pulse height spectrum (PHS) of an actual CC(1x3) mode event list. In this report we investigate the relation of the 1x3 event detection scheme used in CC mode towards the 3x3 island predominantly used in TE mode in terms of QE and the spectral redistribution function (see Figure 2).

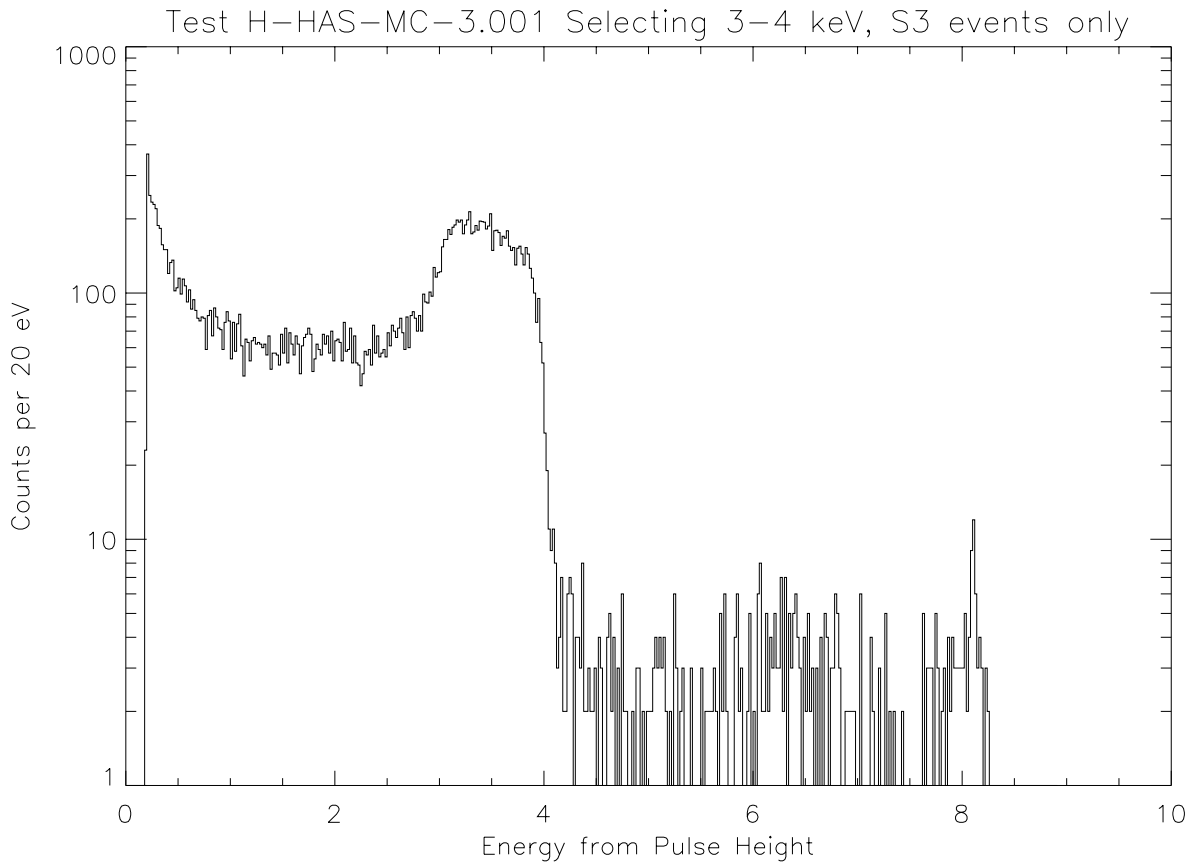

Figure 1. Pulse height distribution (PHD) for a region of the S3 (BI) CCD selected from events whose dispersion corresponds to the 3-4 keV range, assuming $m = 1$ (taken from test H-HAS-MC-3.001). The peak in the 3-4 keV band is expected but the tail that extends to extremely low pulse heights contains much more power than expected. Normally, in timed exposure mode, of order 1% of events would appear in a small peak at 1.74 keV, which is the Si-K escape peak. The escape peak is not visible in this plot because it appears to have been swamped by events with partial charge collection. Note: the peak at 8 keV looks as if it might be due to pile-up, but it is, actually the 2^{nd} order Cu Kα line (8.05 keV).

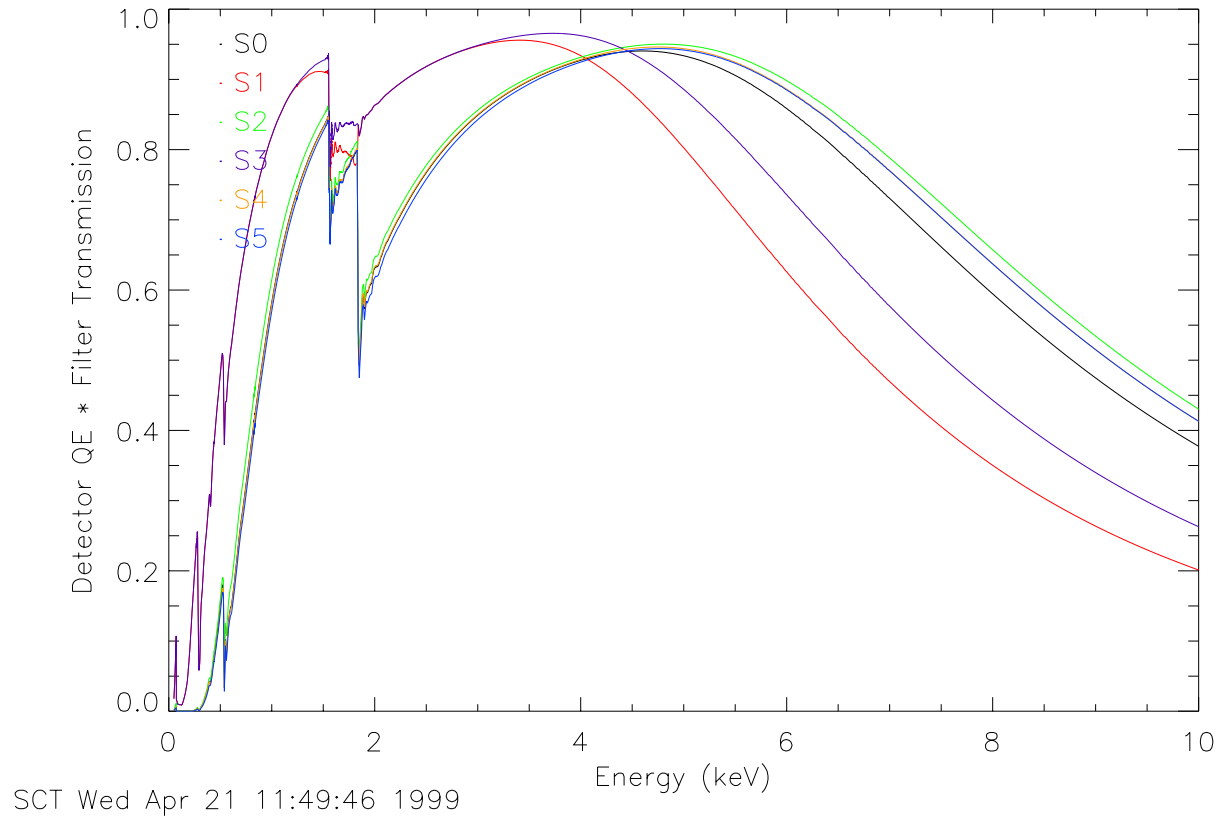

Figure 2. Effective efficiencies (quantum efficiency × filter transmission) as a function of energy each of the ACIS-S detector arrays (courtesy of the MIT ACIS team, August 1998). The curve for chip S4 (in orange) cannot be seen for most of the energy range, because it is very similar to the curve for chip S5 (in blue). These curves represent the average QE over the entire array, and do not include variations in the QE over the array.

In Figure 3, counts were extracted from HETG and LETG data sets, and then divided by the TE mode QE (BI and FI QE templates were used) and the exposure time. If the QE is correct, the ratio of the counts on the BI device to the FI device should be equal to 1. As you can see, this is not the case. This indicates a change in QE in CC mode relative to TE mode.

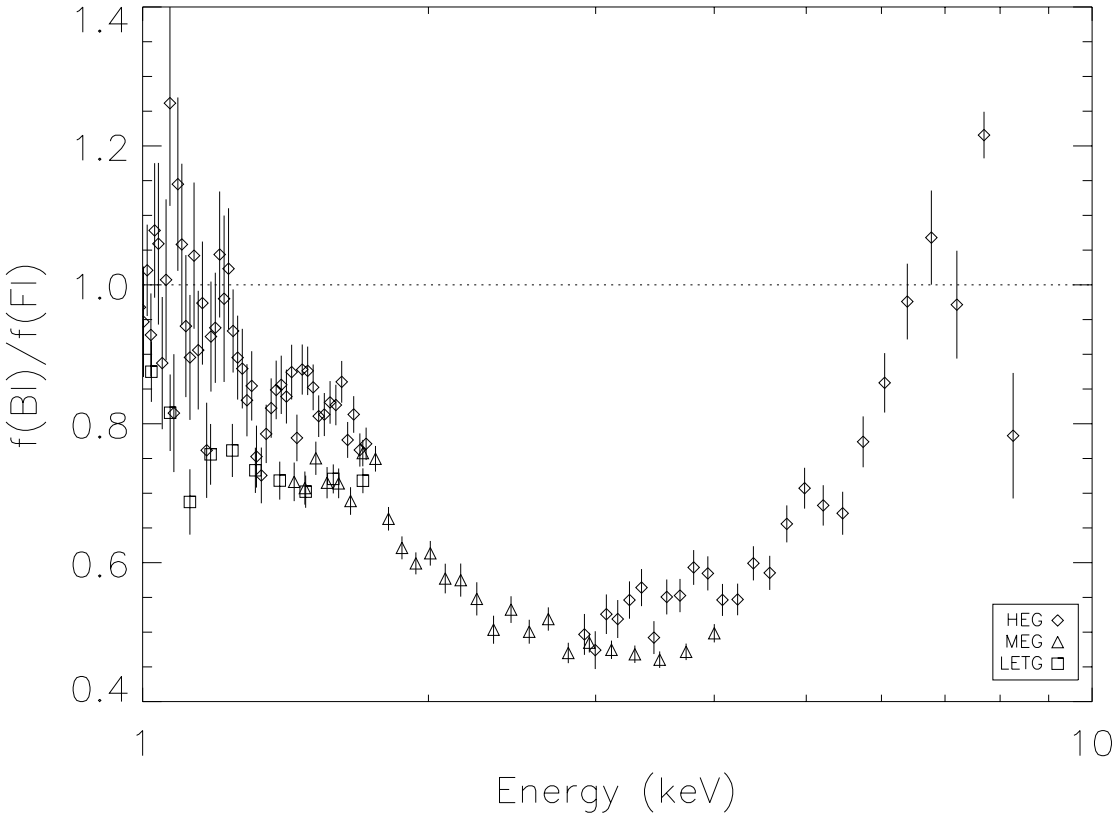

Figure 3. BI/FI flux ratios from Cu anode continuum tests.

2. DATA

For this analysis we used event lists collected at the X-ray Calibration Facility (XRCF) for the HETG effective area calibration.[6,7] The event lists were "converted" to CC mode by splitting each TE mode 3x3 event island into three 1x3 event islands. We applied the standard event thresholds of 38 for the FI devices and 20 for the BI devices, and a split threshold of 13 for all devices. As x-ray sources, the double crystal monochromator (DCM) and four different electron impact point sources (EIPS) were used. All event lists were collected in full HETGS configuration, which includes the High Resolution Mirror Assembly (HRMA), the High Energy Transmission Grating (HETG), and the ACIS-S array. In addition, the detector plane was moved out of focus to reduce pile-up. Tables 1 and 2 list the experiments used for this analysis with the EIPS and DCM, respectively.

TRW-ID H-HAS-EA-	Source	Primary Line	Energy eV
2.001	Al	Kα	1487
6.001	O	Kα	525
6.005	Fe	Kα	6404
6.006	Cu	Kα	8048

Table 1. EIPS measurements used for CC(1x3) mode analysis.

TRW-ID H-HAS-EA-	DCM crystal	Energy eV	Increment eV	steps	~cts/step
8.001	TAP	950	50	5	41000
8.002		1200	50	5	45000
8.003		1400	30	11	28000
8.004		1860	20	8	35000
8.005		2050	30	11	12000
8.006	Ge1	2500	150	11	18000
8.007		4000	200	6	18000
8.008		5000	250	9	28000
8.009		7200	500	4	23000

Table 2. DCM measurements used for CC(1x3) mode analysis.

3. DATA REDUCTION

To extract the events from the dispersed spectrum, we computed the expected position of the event in the detector array based on the dispersion relation

$$sin(\theta) = \frac{m\lambda}{p}, \tag{1}$$

where θ is the dispersion angle, m is the order, λ is the wavelength, and p is the grating period, and selected the events between two concentric rings. See an example spectrum in Figure 4.

In this document we present only the results for the $\pm 1^{st}$ orders, in order to maintain high counting statistics. We also present the results assuming negligible pile-up. For most of the TE mode data, multi-photon pile-up does not significantly contribute to the total counts, but for the higher energy lines, pile-up peaks corresponding to 2, 3, 4 (or more) photons may appear in the pulse height spectrum at 2, 3, 4 (or more) times the expected energy, respectively (see Figure 5). In CC mode, the integration time is generally short enough to avoid the problems due to pile-up; therefore, we included data only from the primary peak in the pulse height spectrum.

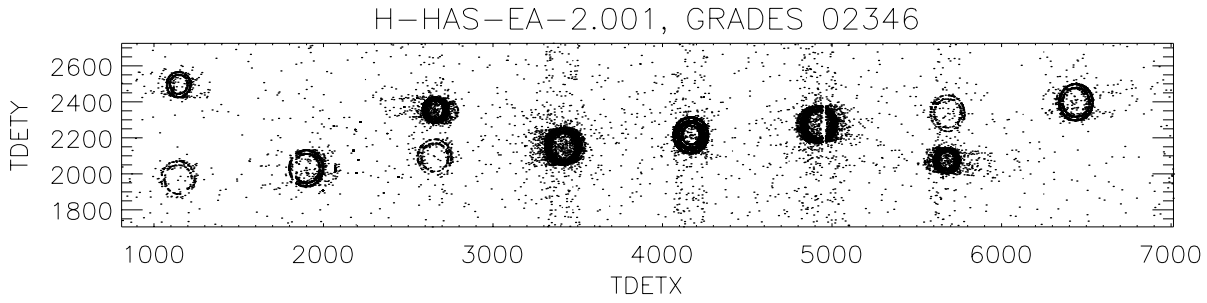

Figure 4. An example of a defocused, dispersed spectrum. These data are from H-HAS-EA-2.001, using the Al EIPS source. The 0^{th} order is visible at an X position (in tiled detector coordinates) of about 4100. Lines from the Medium Energy Grating (MEG) can be seen to the lower left and upper right of the 0^{th} order, and lines from the High Energy Grating (HEG) can be seen to the upper left and lower right. The 1.4 keV energy line can be seen out to fourth order for the MEG grating on the negative side.

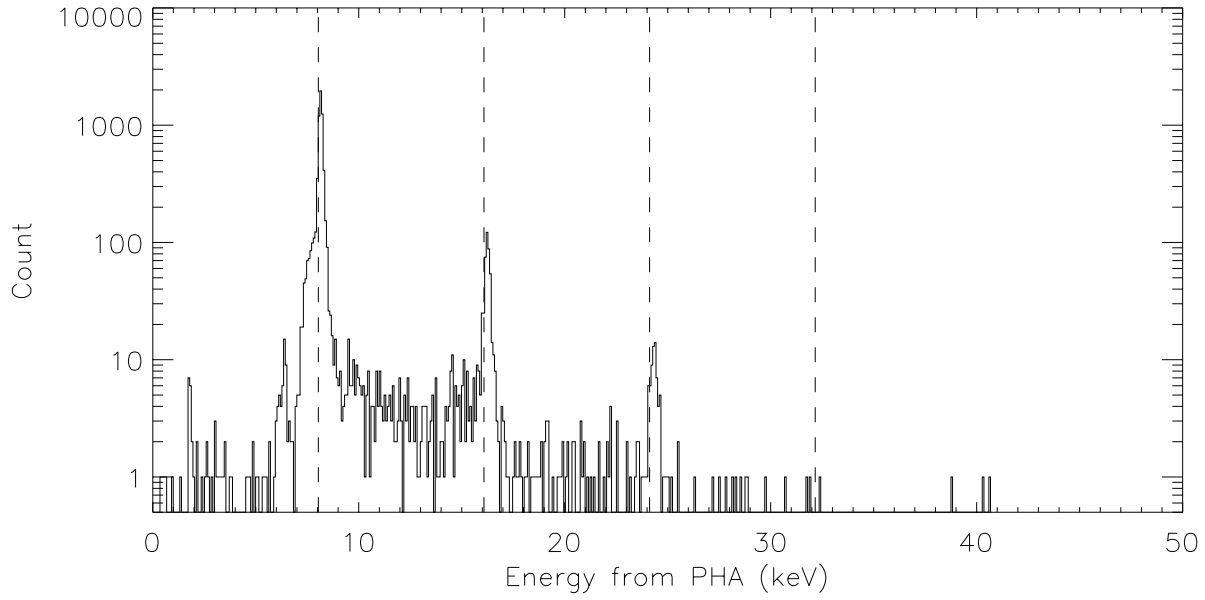

Figure 5. An example of a piled-up spectrum. These data are from H-HAS-EA-6.006, taken in TE mode, and using the Cu EIPS source. The $+1^{st}$ order line from the HEG has been extracted to create this energy spectrum. The primary peak at 8.048 keV, and the three pile-up peaks are labeled with dashed lines.

To reduce the data, we first selected events based on their TE mode grade, using the standard ASCA grades 0, 2, 3, 4, and 6. Figure 6 illustrates these 5 standard and the 3 non-standard ASCA grades*. Then, in order to create CC mode events out of each of the TE events, we split each 3x3 event island into three 1x3 events, using the standard event thresholds of 20 for BI devices and 38 for FI devices, and a split threshold of 13. From these events, we accepted only CC mode grades 0, 3, and 4. Figure 7 illustrates these grades.

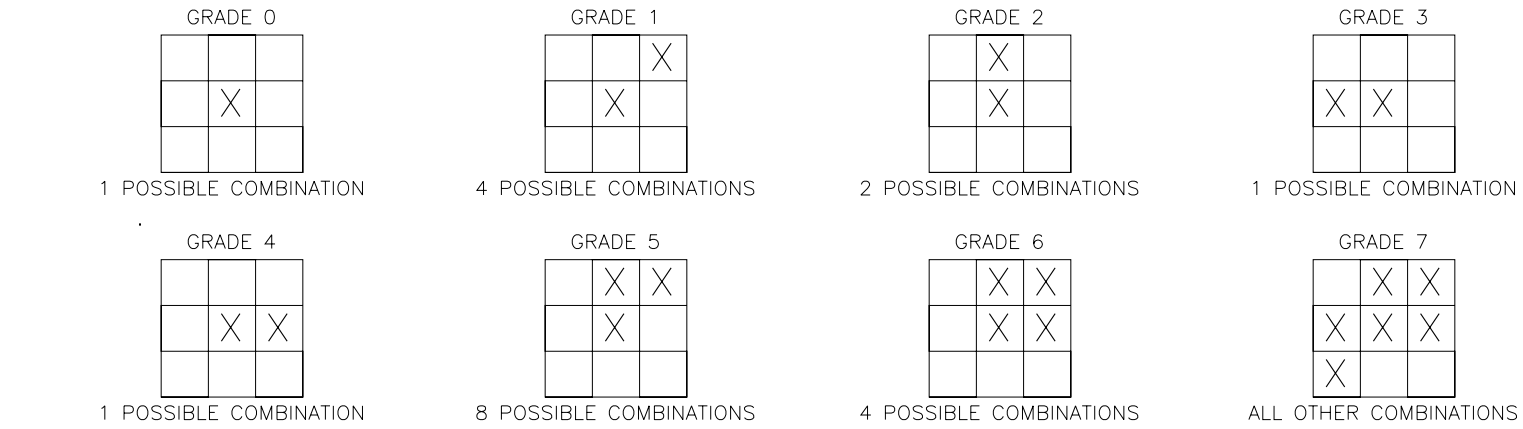

Figure 6. Grades in Timed Exposure mode. The squares with an "X" in them represent a pixel which is at or above above the split threshold of 13, and blank squares represent pixels which are below the split threshold.

Figure 7. Grades in Continuous Clocking 1x3 mode. The squares with an "X" in them represent a pixel which is at or above above the split threshold of 13, and blank squares represent pixels which are below the split threshold.

The reader should note that the CC mode grades 0, 3, and 4 are defined in the exact same way as for TE mode. Therefore, the CC mode grades selected are a direct subset of the TE mode grades, eliminating only grades 2 and 6 from the standard grade set. When one of these two grades (2 or 6) in TE 3x3 mode is split into three rows, the middle row will automatically become a grade 0, 3, or 4 in CC mode. Additionally, if one or more of the pixels in the row above or below it is above the event threshold, then it will also be registered as an event by the detection software. Figure 8 shows an example of how a grade 6 event in TE mode can be split into two grade 4 events in CC mode.

The last step was to compute an energy for the CC mode events. This was calculated using the same conversion factor as for the TE mode events.

$$\mathrm{E}_{CC} = \left(\frac{\mathrm{E}_{TE}}{\mathrm{PHA}_{TE}}\right) \mathrm{PHA}_{CC} \tag{2}$$

There are two potential problems associated with collecting data in CC mode. The first is the loss of charge in the middle row of the event, created by splitting off the rows above and below it. The second is the charge in the adjacent rows or the charge in rows split from the non-standard grades (1, 5, and 7), which may show up as false events if one of the pixels is above the event threshold. Both of these have been observed in actual CC mode pulse height spectra as a shift in the peak centroid and a higher tail (See Figure 1). For a quantitative analysis of these effects, we have treated these two issues separately.

*Strictly speaking, there are more possible combinations for most grades than are listed in Figure 6. There are some special rules for grading when a corner pixel is above the split threshold, but these cases are not included here for simplicity. For a complete description of the ACIS grading scheme, the user is referred to References.[3,4]

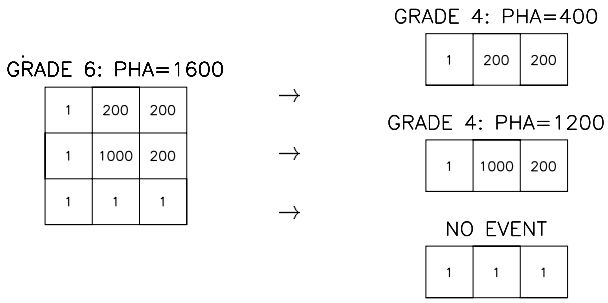

Figure 8. An example of how a grade 6 event in TE mode can be split into two grade 4 events in CC(1x3) mode. The number in each square is the pulse height amplitude (PHA) in analog data units (ADU).

3.1. Lost Charge

For each extracted line, two pulse height spectra were created from the two sets of selected events, using all events in TE mode, and the CC mode events which came from middle row of the 3x3 event. The peak in each was then fit to a gaussian in order to characterize the general peak properties as a function of energy and chip (see Figure 9).

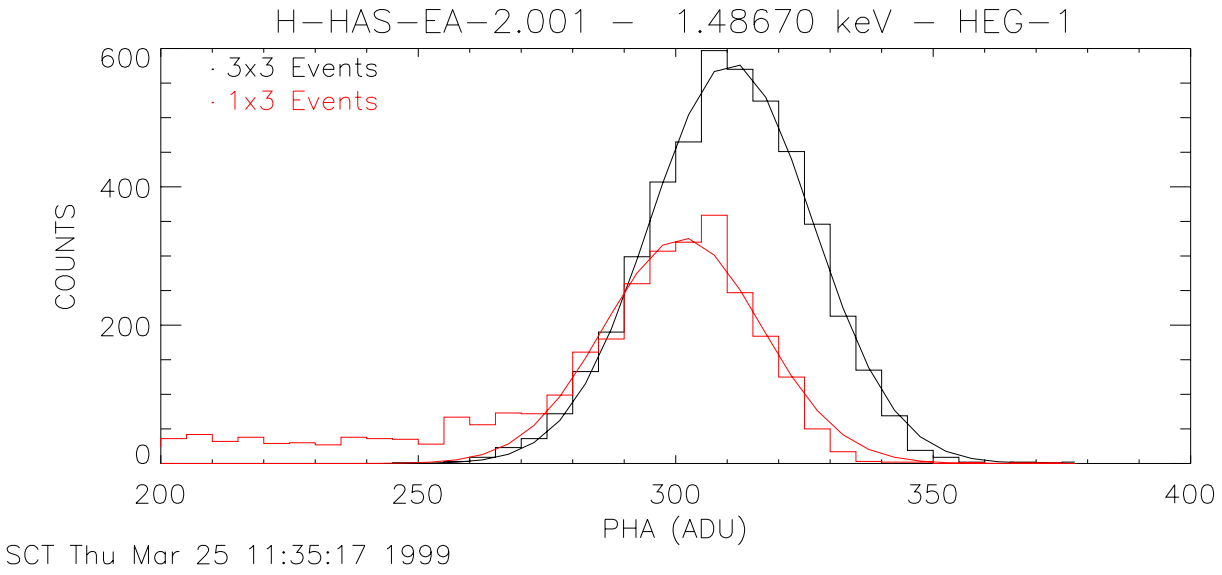

Figure 9. An example of the two binned spectra from TE mode events and "middle" CC(1x3) mode events. Each peak has been fit to a gaussian function.

The overlap of the two peaks is also of special interest, because there may be a significant shift in the centroid of the gaussian. To investigate this further, we used two methods. First, we defined several bandpasses around the centroid of the TE peak and counted the number of CC mode and TE mode events within that energy range (see Figure 10). We used bandpasses of ±80 eV, ±100 eV, ±120 eV, ±140 eV, and ±160 eV. Because the QE in TE mode has been well characterized, the ratio of TE mode events to CC mode events within a given bandpass will give a correction factor for the QE in CC mode. This will be useful for analyzing CC mode data in-orbit. Second, we used the same upper energy limits and decreased the lower energy limit until the bandpass contained the same number of CC mode and TE mode counts. This gives us information on how events are redistributed in energy when using CC mode, compared to TE mode, and how large of an energy range we need to return to the original (TE mode) QE.

3.2. False Events

Figure 8 shows how a TE mode (3x3) event is split into three CC mode (1x3) events. The bottom row does not register as an event in CC mode, because all three pixels are below the event threshold. The middle row is what we

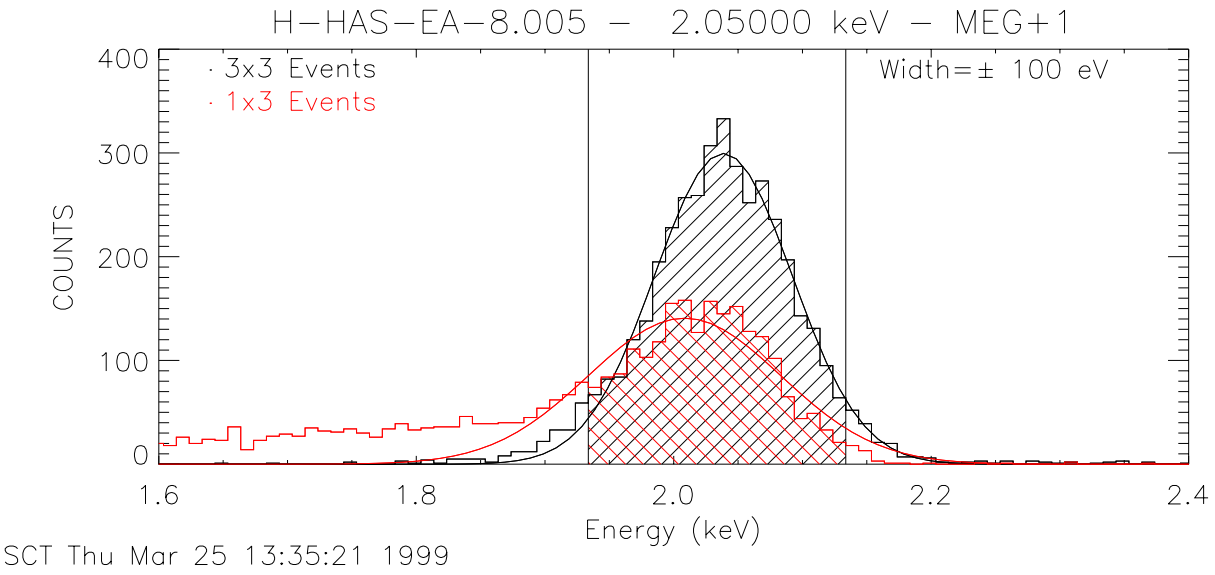

Figure 10. An example of the peak overlap between CC(1x3) and TE modes. Each peak has been fit to a gaussian function, and then events were selected by a bandwidth around the centroid of the TE peak.

define as an "actual event", because it contains the pixel with the greatest charge. Therefore, it's total charge, in most cases, will be the closest to the total charge in TE mode event (1200 ADU, compared to 1600 ADU). The top row is an example of a "false event". It has at least one pixel that is above the event threshold, and is registered as an event, but its total PHA is lower than the actual event (400 ADU). These events will artificially increase your QE. However, this is only a significant problem if the energies of these false events are large enough to be confused for an actual event.

Another example of how false events can be created is shown in Figure 11, where a grade 7 in TE mode is split into 2 grade 4 and 1 grade 0 events in CC mode. With increasing energy and count rate, events tend to "migrate" into higher number grades. Therefore, the number false events from these grades is energy and count rate dependent. The energy dependent component is caused by the charge cloud from a single event covering more pixels. This effect should also be visible in actual CC mode data. The count rate dependent component is caused by overlapping charge clouds from more than one event within an integration cycle. Because of the shorter integration times in CC mode, this component should not be present in actual CC mode data. In the data that were used for this analysis, it is the count rate dependent component of grade migration that dominates. Therefore, we have excluded the non-standard TE mode grades when calculating the number of false events, and kept only the false events from grades 2 and 6. As a result, the number of false events may be underestimated. It should also be noted that there will be a count rate dependent component present in the number of false events from grades 2 and 6, but this should be offset by underestimation caused by eliminating grades 1, 5, and 7 from the calculation of the number of false events. For a full description of grade migration and its energy and count rate dependence, please refer to References.[1,7]

Again, we took two approaches to analyze the effect of false events. First, we calculated the percentage of false events as a function of energy for each chip. In this approach, we needed to know, not only the relative abundancy of the false events, but also if their energies were large enough to be confused for actual events. So, for each extraction bandwidth described in section 3.1, we computed the number of false events within it, to see if there was an overlap in energy between the actual and false events. Second, we gradually raised the values of the event thresholds from the standard 38 for FI and 20 for BI, to see how much that would effect the results.

4. ANALYSIS AND RESULTS

4.1. Lost Charge

Figures 12 and 13 show the results of fitting the TE and CC mode pulse height peaks. The order of the plots are the: difference in total peak area (UL), peak centroid shift (UR), difference in peak height (LL), and difference in

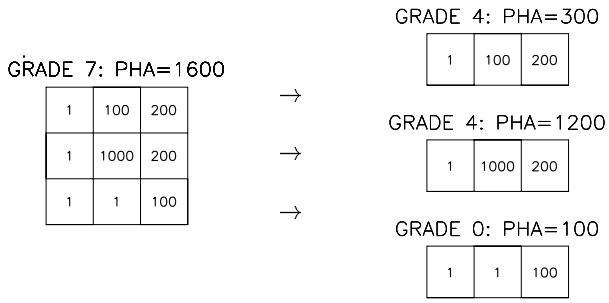

Figure 11. An example of how a grade 7 event in TE mode can be split into two grade 4 and 1 grade 0 events in CC(1x3) mode. The number in each square is the PHA in ADU.

standard deviation (peak width) (LR), all plotted versus energy. The peak area was calculated by integrating the gaussian fit for each line over all energies, and the three other values are the gaussian fit parameters. In both sets of plots, there is a different color used for each chip, where S4/S5 refers to lines which span the gap between chips S4 and S5.

For the BI chips, these results imply a shift in the centroid energy in CC mode with respect to TE mode. However, in the case of the FI CCDs, the centroid shifts are all less than 1 ADU, and, therefore not significant. The largest difference for both devices is in the peak height, which causes the reduction in peak area. The amount of the peak area reduction can be interpreted as a measure of the reduction in quantum efficiency, which is maximum of 45% at 3 keV for the BI chips, and steadily increasing with increasing energy from 5% to 45% for the FI devices.

One of the most striking features in these plots, especially those for the FI chips, is the jump at the Si K edge, near 1.8 keV. For FI devices, there is a smaller difference in peak height and peak area just above the edge, when compared to just below the edge. An effect is also seen in the ACIS QE curves at this energy. In the BI chips these effects are much less pronounced, which should be attributed to the fact that, because of its fundamentally different design, absorption at Si-K is much weaker in BI devices and the Si-K edge appears very weak in the TE QE (see Figure 2).

Figures 14 through 16 show peak overlaps at various bandwidths in TE and CC mode, for each chip. Figure 14 shows the percentage of all extracted counts in CC mode, which are within the given bandpass around the TE mode centroid, compared to the extracted counts in TE mode, within the same bandpass. Figures 15 and 16 show the percentage of all extracted counts in CC and TE modes, respectively, which are within the given bandpass around the TE mode centroid.

Again, we observe an effect at the Si-K edge for all three plots. In Figures 14 and 16 the effect appears as a jump of about 7%, and in Figure 15, as a change in slope.

Figure 14 represents the change in quantum efficiency of CC mode compared to TE mode. For FI chips, the CC to TE ratio starts at about 95% agreement for low energies and, aside from the jump at the Si edge, steadily decreases with increasing energy to about 55% at 8 keV. For BI chips, the ratio is about 80% for the O Kα line at 525 eV, and decreases to about 50% at 3 keV, where it begins to increase again, up to about 60% at 8 keV.

Tables 3 through 10 in Appendix A list the values shown in Figure 15. That is, the percentage of CC mode counts within the given bandwidth about the TE mode centroid, for each chip.

For the results shown in Figures 17 through 19, we used upper energy bandwidths of +80 eV, +100 eV, +120 eV, +140 eV, and +160 eV, and lowered the low energy limit until the number of events in CC mode was at least 66.7%, 85%, and 95%, respectively, of those in TE mode. Again, the bandwidths are referenced to the TE mode peak centroid. These figures show how large of an energy range you need to get back to the given percentage of the original (TE mode) QE.

As it turns out, in the cases of 66.7% and 85% the lower bandwidth limits stay the same as the higher limits throughout most of the applicable energy range in S1, S4, and S5, which however never exceed 3 keV. S2 and S3 cover much larger portions of the bandpass and we observe that, in the case of S2 that at higher energies and S3

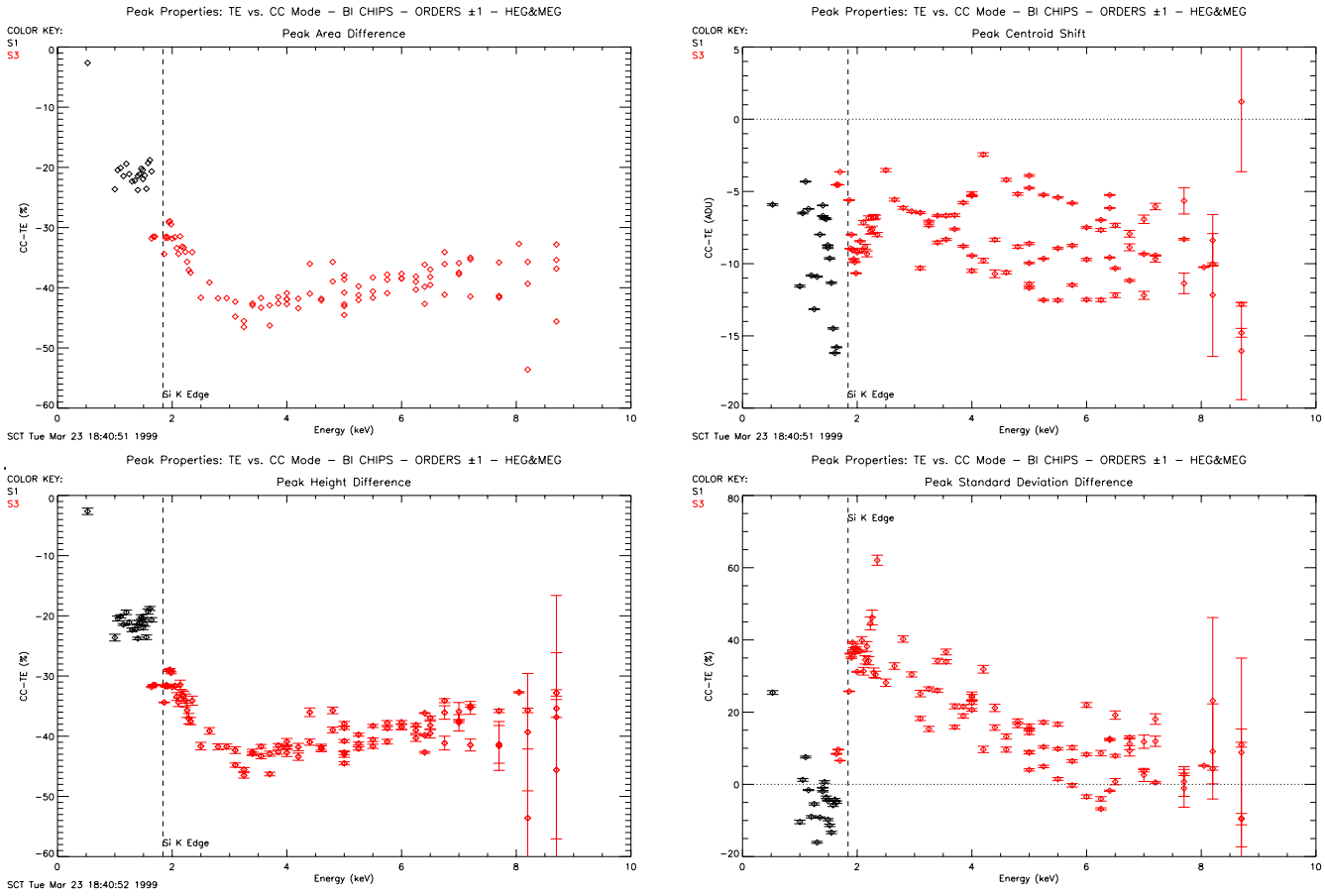

Figure 12. Difference in overall peak area (integrated using gaussian fit), centroid shift, difference in peak height, and difference in peak standard deviation (all from fit parameters) between TE and CC(1x3) modes on the BI chips. The error bars on the plots for centroid shift, difference in peak height, and difference in peak standard deviation are the uncertainties in each fit parameter.

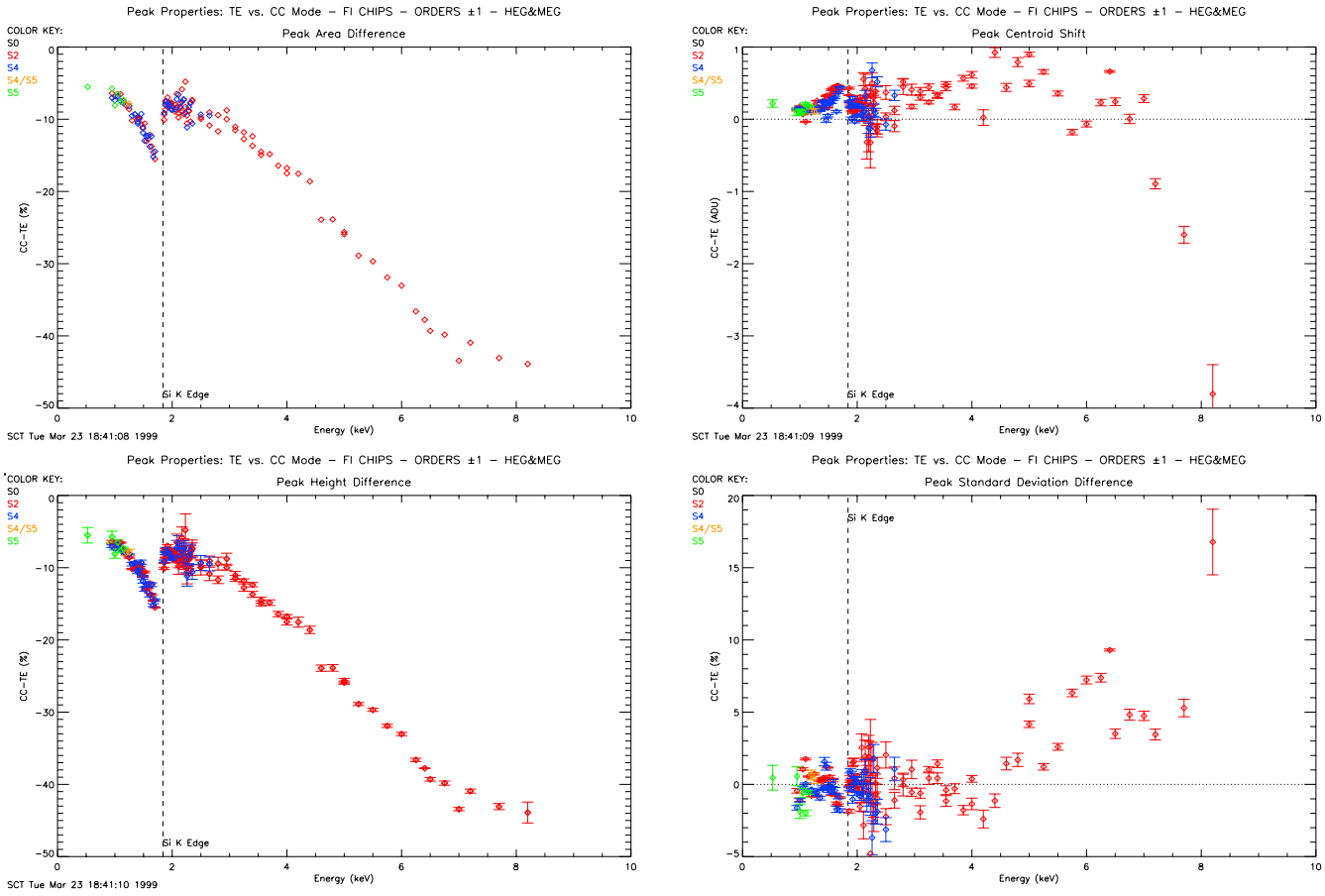

.

Figure 13. Difference in overall peak area (integrated using gaussian fit), centroid shift, difference in peak height, and difference in peak standard deviation (from fit parameters) between TE and CC(1x3) modes on the FI chips. The error bars on the plots for centroid shift, difference in peak height, and difference in peak standard deviation are the uncertainties in each fit parameter.

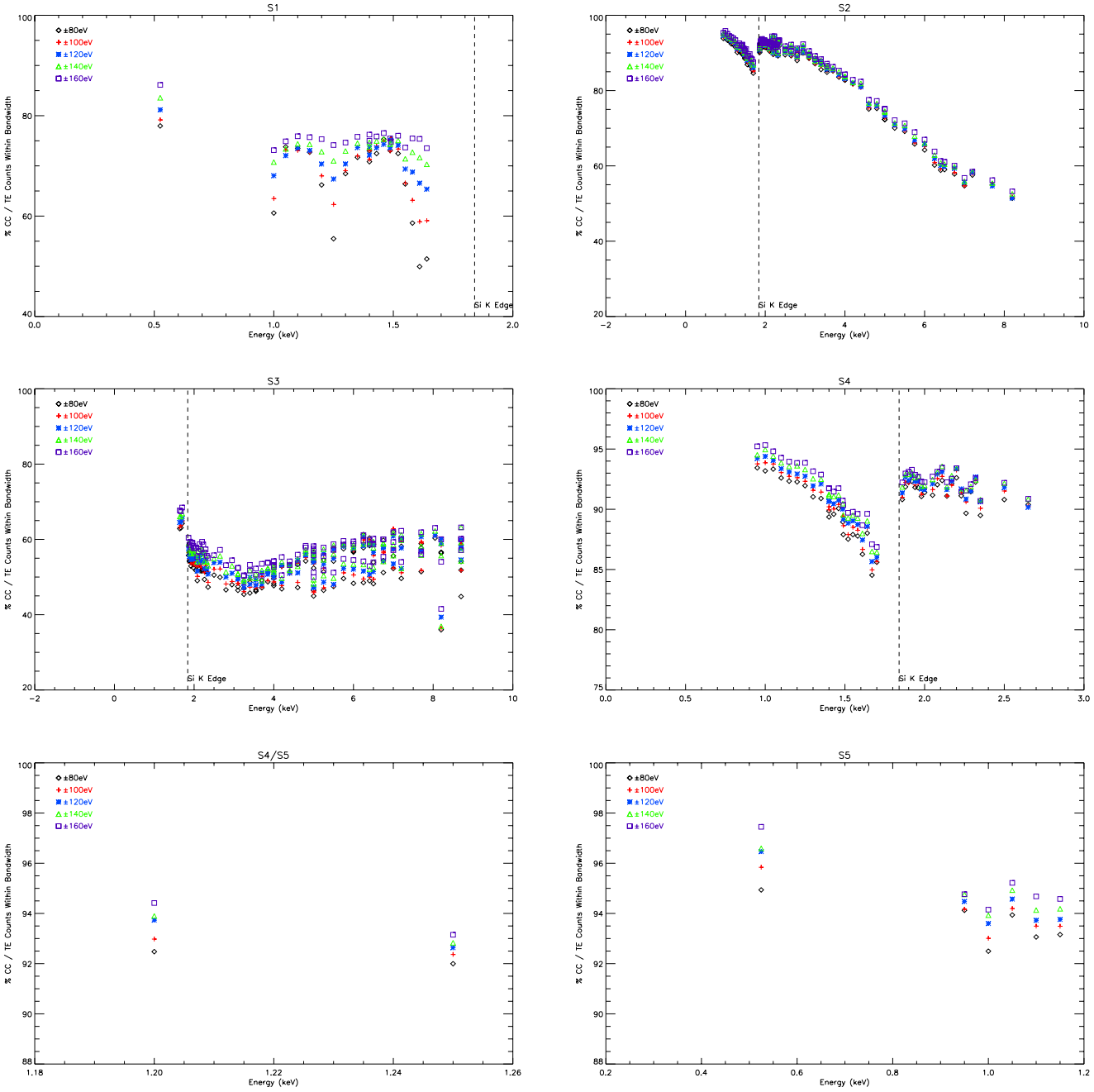

Figure 14. The percentage of extracted counts in CC(1x3) mode to the extracted counts in TE mode, within the listed bandpass around the TE mode centroid, separated by chip ($100 \times (CC(E_0 - \Delta E < E < E_0 + \Delta E)/TE(E_0 - \Delta E < E < E_0 + \Delta E))$). There is a different symbol and color used for each bandpass; black $\diamond$ for $\pm$80 eV, red $+$ for $\pm$100 eV, blue $*$ for $\pm$120 eV, green $\triangle$ for $\pm$140 eV, and purple $\square$ for $\pm$160 eV.

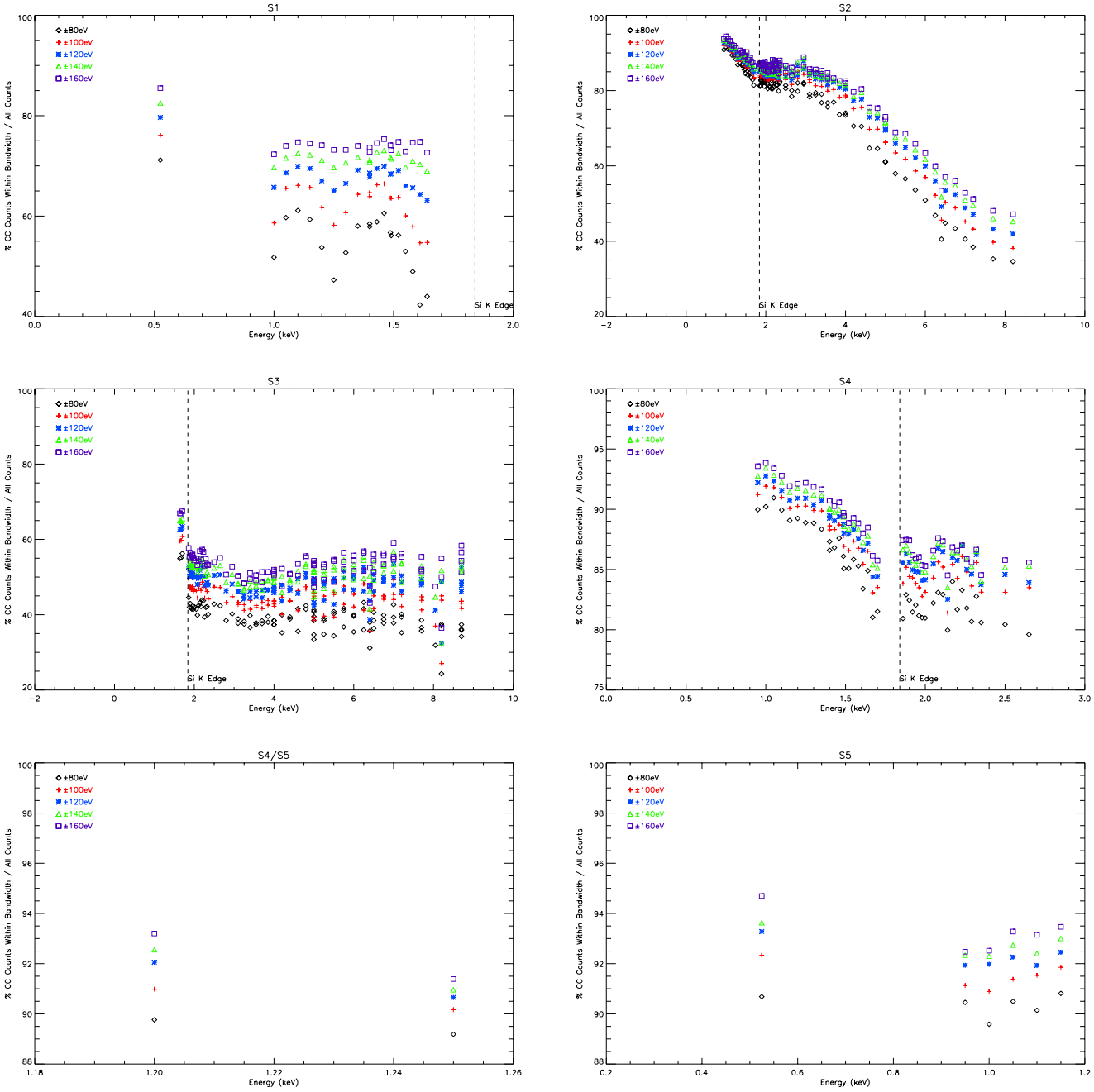

Figure 15. Percent of all extracted counts in CC(1x3) mode, which are within the listed bandpass around the TE mode centroid, separated by chip ($100 \times (CC(E_0 - \Delta E < E < E_0 + \Delta E)/TE(AllE))$). There is a different symbol and color used for each bandpass; black $\diamond$ for ± 80 eV, red $+$ for ± 100 eV, blue $*$ for ± 120 eV, green $\triangle$ for ± 140 eV, and purple $\square$ for ± 160 eV.

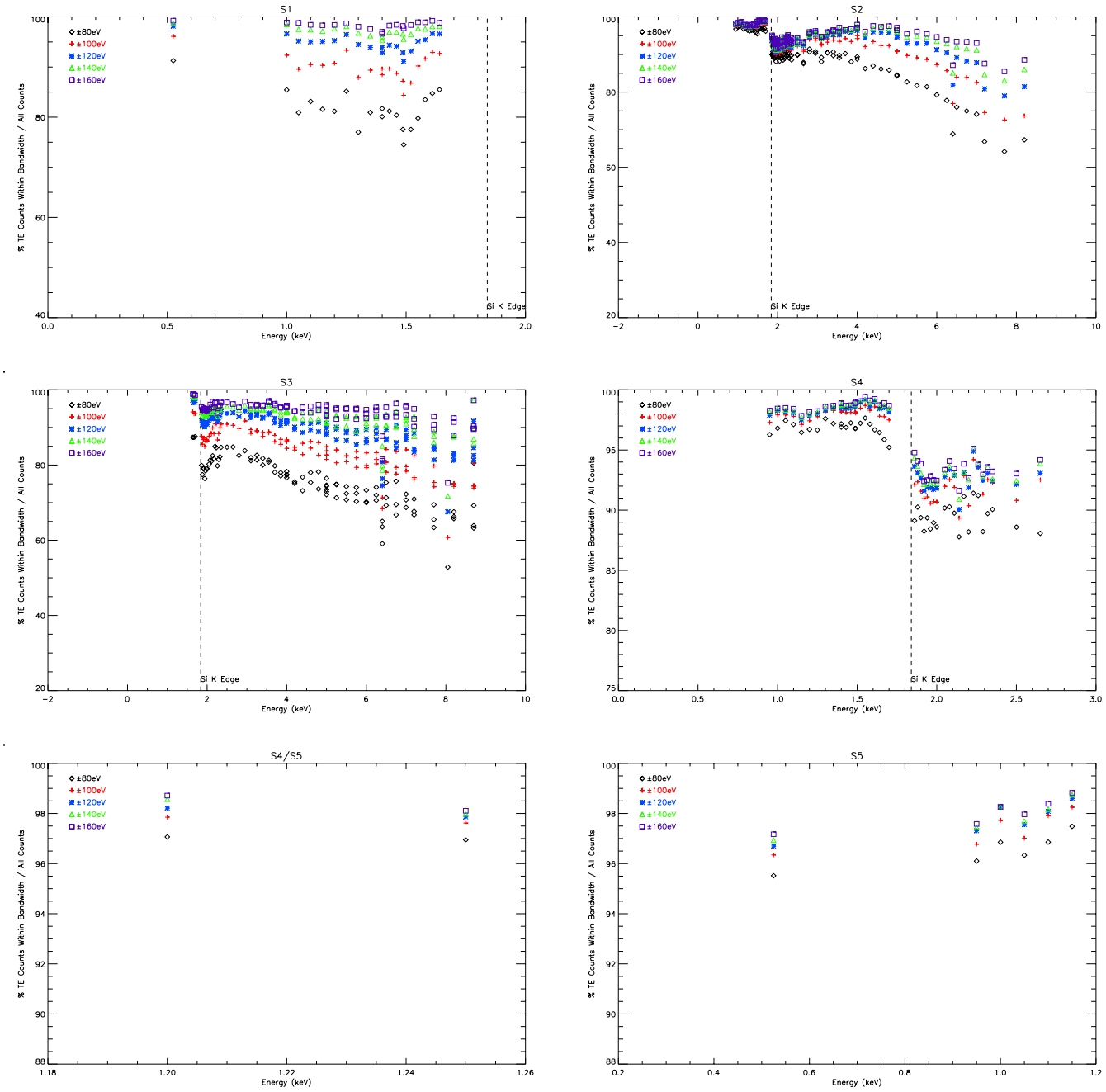

Figure 16. Percent of all extracted counts in TE mode, which are within the listed bandpass around the TE mode centroid, separated by chip $(100 \times (TE(E_0 - \Delta E < E < E_0 + \Delta E)/TE(AllE)))$. There is a different symbol and color used for each bandpass; black $\diamond$ for ± 80 eV, red $+$ for ± 100 eV, blue $*$ for ± 120 eV, green $\triangle$ for ± 140 eV, and purple $\square$ for ± 160 eV.

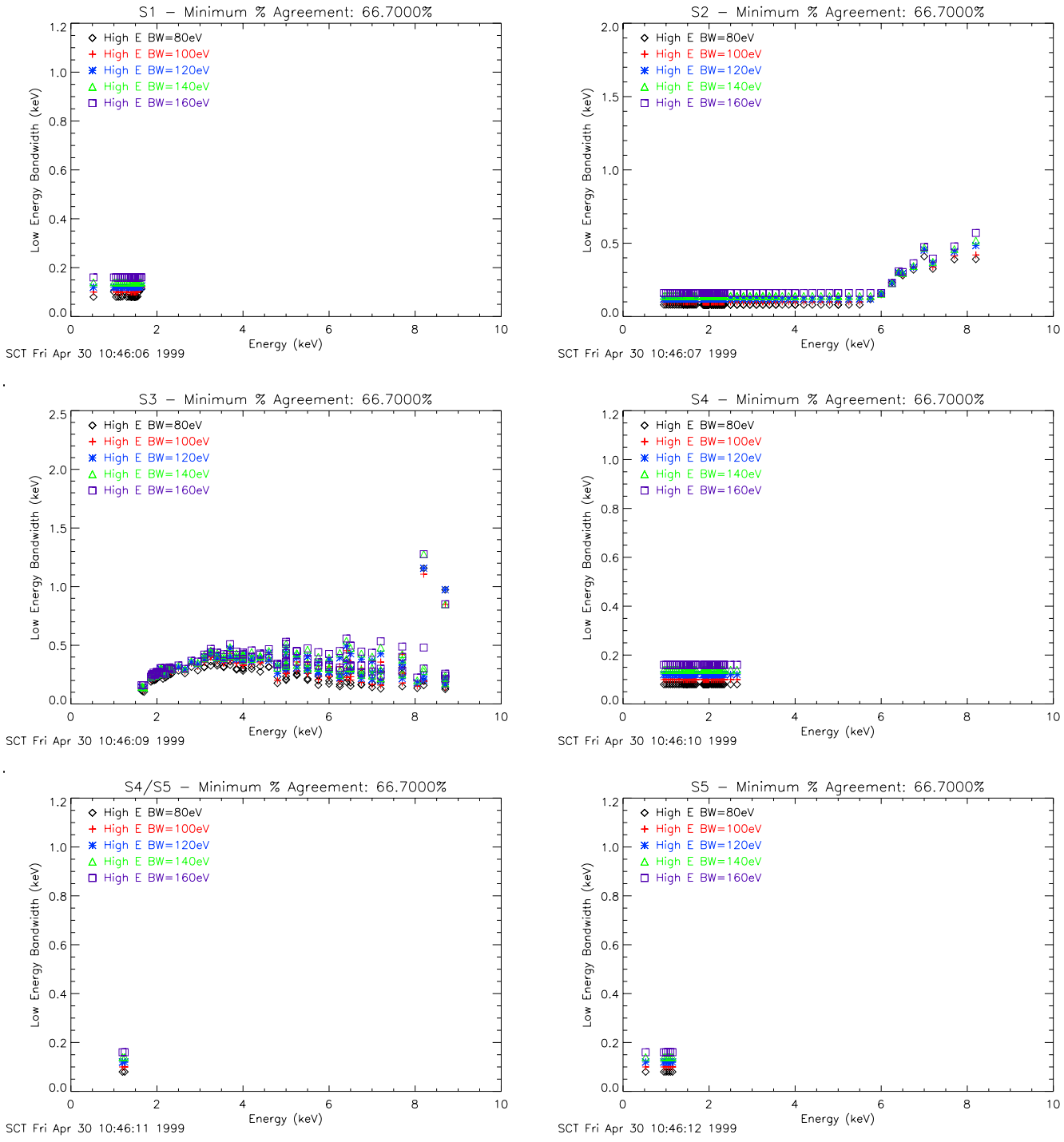

Figure 17. The lower energy bandwidths for various upper energy bandwidths, where the number of counts extracted in CC(1x3) and TE modes match with a minimum of 66.7%. There is a different symbol and color used for each upper energy bandwidth; black $\diamond$ for +80 eV, red + for +100 eV, blue $*$ for +120 eV, green $\triangle$ for +140 eV, and purple $\square$ for +160 eV.

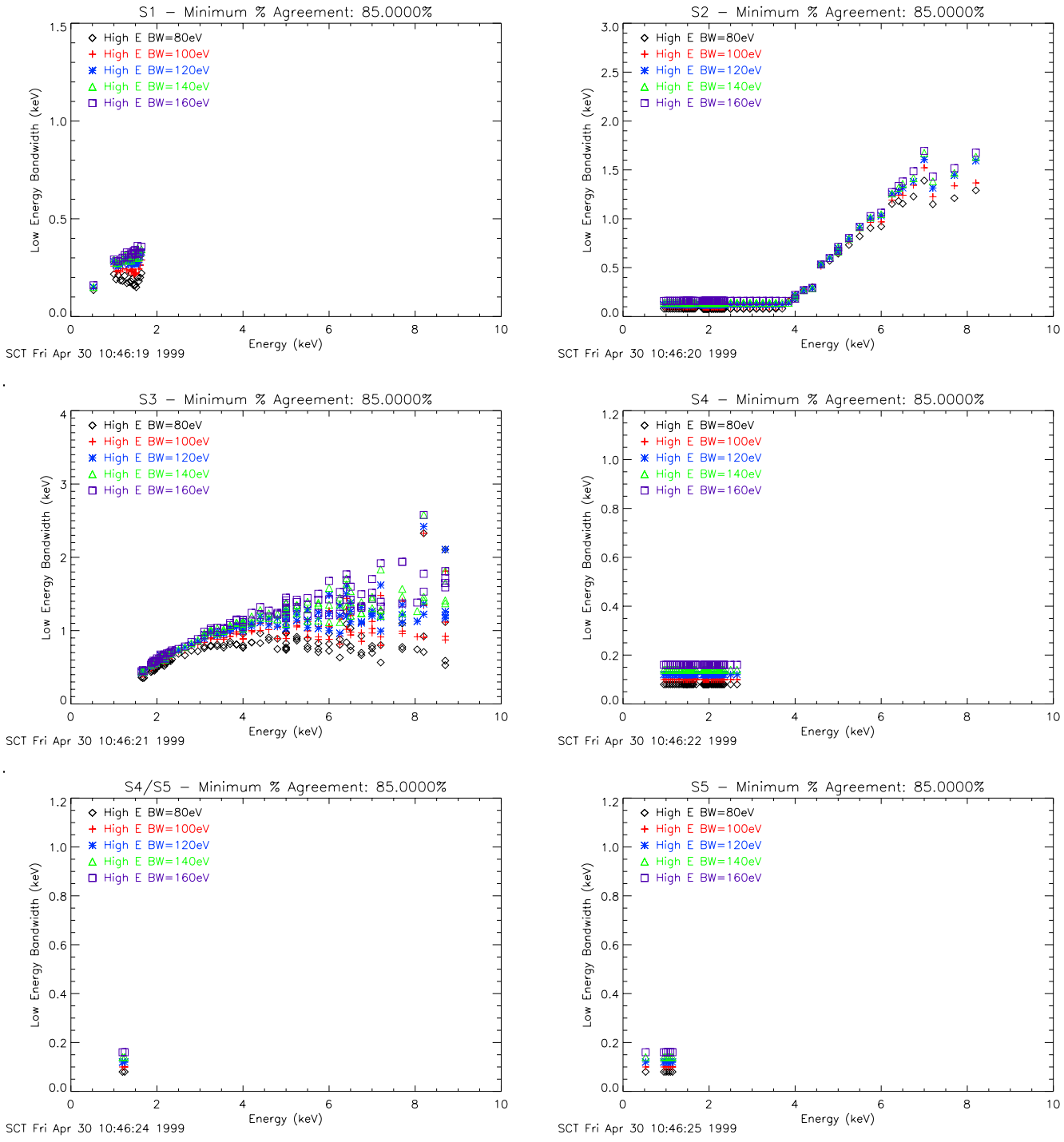

Figure 18. The lower energy bandwidths for various upper energy bandwidths, where the number of counts extracted in CC(1x3) and TE modes match with a minimum of 85%. There is a different symbol and color used for each upper energy bandwidth; black $\diamond$ for +80 eV, red + for +100 eV, blue $*$ for +120 eV, green $\triangle$ for +140 eV, and purple $\square$ for +160 eV.

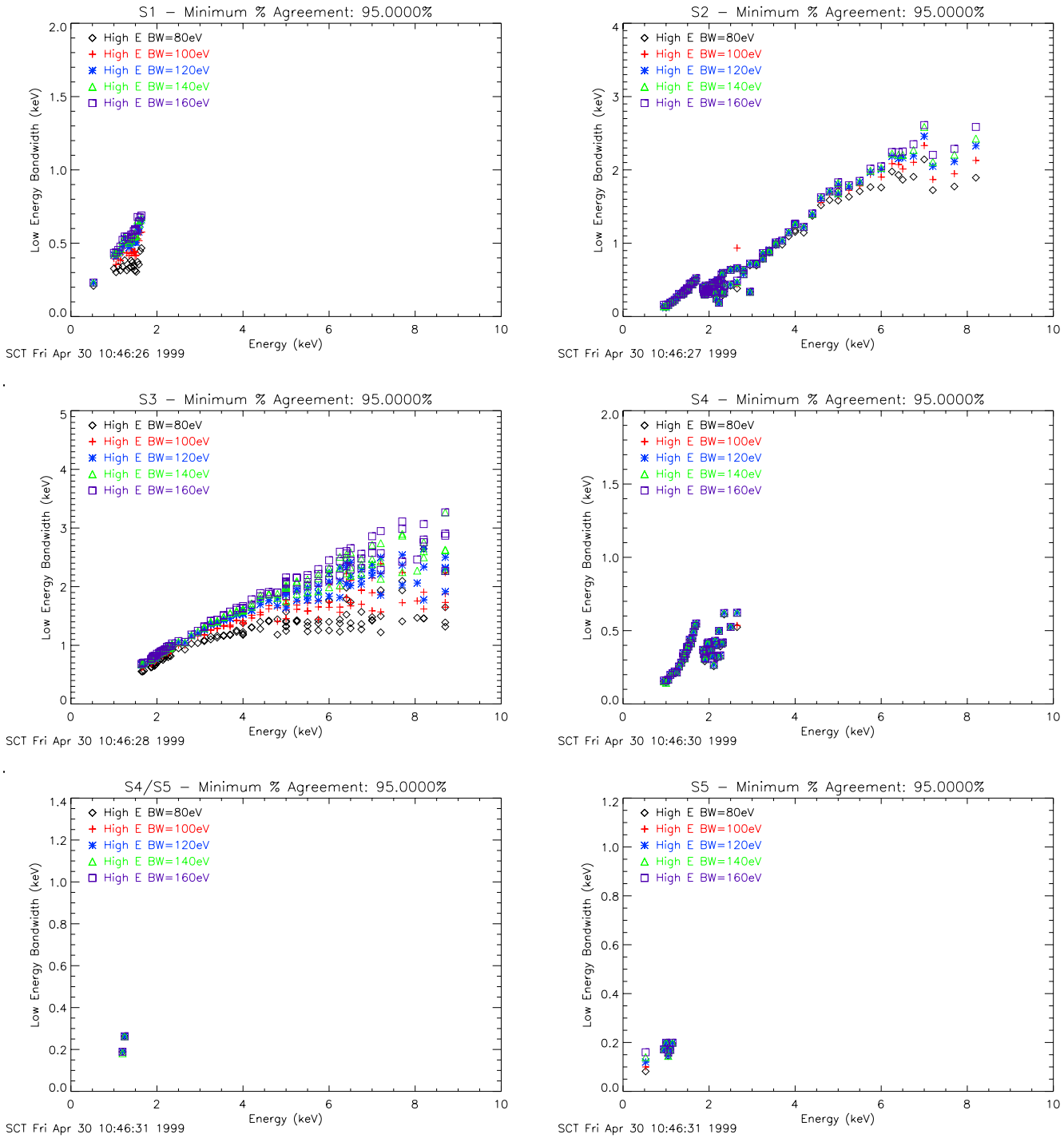

Figure 19. The lower energy bandwidths for various upper energy bandwidths, where the number of counts extracted in CC(1x3) and TE modes match with a minimum of 95%. There is a different symbol and color used for each upper energy bandwidth; black $\diamond$ for +80 eV, red + for +100 eV, blue $*$ for +120 eV, green $\triangle$ for +140 eV, and purple $\square$ for +160 eV.

for all energies, the lower limits have to be increased in order to include all the charge. For the 95% case the lower bandwidth limit is always larger than the higher limit in all devices.

In Figure 17, the plots for all energies in S1, S4, S4/S5, and S5, and for energies below 5.5 keV in S2, the lower energy bandwidth was the same as the upper limit, which means that, for each of these plots, a symmetric extraction region about the TE mode centroid is sufficient to extract at least 66.7% of the TE mode events in CC mode. Above 5.5 keV in S2, the lower energy bandwidth increases to about 500 eV at 8 keV. For the S3 plot, at about 1.6 keV this value is about 100 to 150 keV, and increases with increasing energy to a maximum of about 400 eV at 3.5 keV, and then decreases again. The variability of the data also increases with increasing energy.

In Figure 18, again, the plots for all energies in S4, S4/S5, and S5 (the lowest energies), and below energy 4 keV in S2, the lower energy bandwidth was the same as the upper limit. For the other plots, S1, S2, and S3, the variability in the data is increased with increasing energy. For plot S1, where the energy range is small, the lower energy bandwidth is between 150 eV and 350 eV. For energies above 4 keV for S2, it increases with increasing energy to about 1.5 keV at 8 keV, and for the S3 plot, it is about 400 eV at 1.6 keV, and increases steadily with increasing energy to about 1 keV (with a variability of $\pm$400 eV) at 5 keV, where it levels off.

In Figure 19 we can again see an effect at the Si-K edge at 1.8 keV for chips S2 and S4. For each plot, there is generally an increase in the size of the extraction bandwidth with increasing energy, but at 1.8 keV, there is a sharp drop. After this drop, the data continues to increase in value and variability with energy.

Tables 11 through 18 in Appendix B list the lower energy limits for fixed upper energy limits at +80 eV, +100 eV, +120 eV, +140 eV, and +160 eV, for which the total number of counts in CC mode matches that of TE mode (100% agreement).

4.2. False Events

Figures 20 and 21 show the percentage of false events, compared to the total number of events. These events are from the top and bottom rows of the TE 3x3 event island in the standard TE mode grades, first using the standard event thresholds (Figure 20), and then increasing these thresholds to observe the threshold dependence (Figure 21). Figure 21 also shows the percentage of actual events which are lost due to raising the event thresholds.

In Figure 20, where standard event thresholds were used, at the O Kα line at 525 eV, 3% of the total counts in CC mode were due to false counts for FI chips (S5) and 17% for BI chips (S1). The percentage of false counts steadily increases with increasing energy to 11% for FI chips and about 33% for BI chips, just below the Si edge at 1.8 keV. Above the edge, we observe a drop in false events from 11% to 6% for FI chips and a change in slope for BI chips. The percentage of false events for the FI chips then steadily increases with increasing energy to about 45% at 8 keV. The BI chips level off near 3 keV to about 35%, and remain at that level.

Figure 21 shows how the number of false and actual events decrease when we increase the event thresholds from the standard 20 BI, 38 FI to 40 BI, 76 FI. The variability in the number of false events on chip S1 is greatly reduced, and the total percentage of false events is decreased by a few percent for all chips. Also, instead of a change in slope at the Si edge on the BI chips, we observe a jump in the number of false events by about 5%. The largest percentage of actual events that are lost using these thresholds is only 4.1% (FI) and 2.0% (BI) at 525 eV. This generally decreases with increasing energy, except for a jump at the Si edge for FI devices. When the thresholds are increased above these values, there are generally small drops in the number of false events, but the number of actual events lost quickly jumps to 100% at 525 eV. Therefore, raising the event thresholds for CC mode data will not provide a significant benefit.

Figure 22 shows the number of false events that are extracted when using the extraction regions shown in Figure 19, for a 95% match in counts between CC and TE modes. For all energies, chips, and extraction bandwidths, the contamination from false events within those bandwidths is less than 0.5%. For QE agreements of 66.7% and 85% (Figures 17 and 18), the contamination is zero for almost all cases. Therefore, even though the maximum number of false events is 35% (Figure 20, chip S3, E>3 keV), the energies of these events are generally low enough not to be mistaken for actual events.

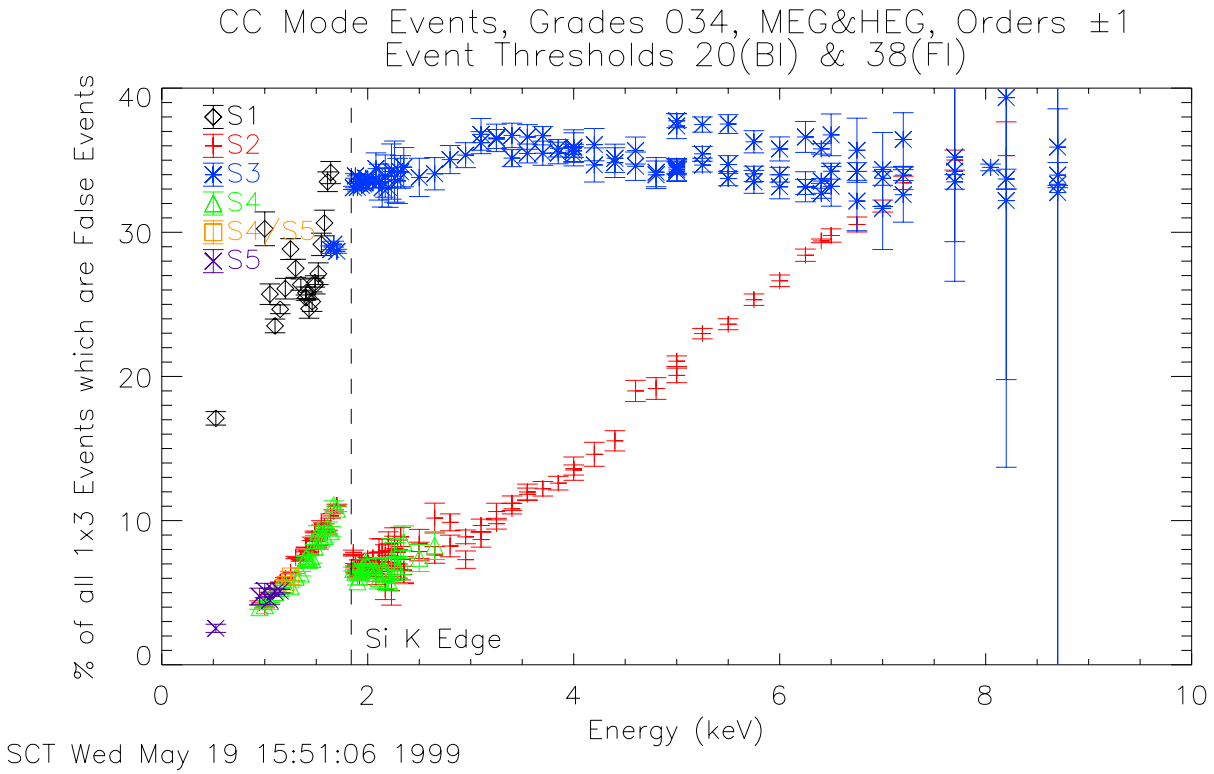

Figure 20. Percent of CC(1x3) mode events which appeared in the top or bottom row in the TE 3x3 event island, compared to the total CC(1x3) mode events from all rows (CC(rows 1,3)/CC(rows 1,2,3)). Standard event thresholds were used to determine if there was an event in the top or bottom rows (20 BI, 38 FI). The error bar on each point is the error derived from the statistical uncertainty.

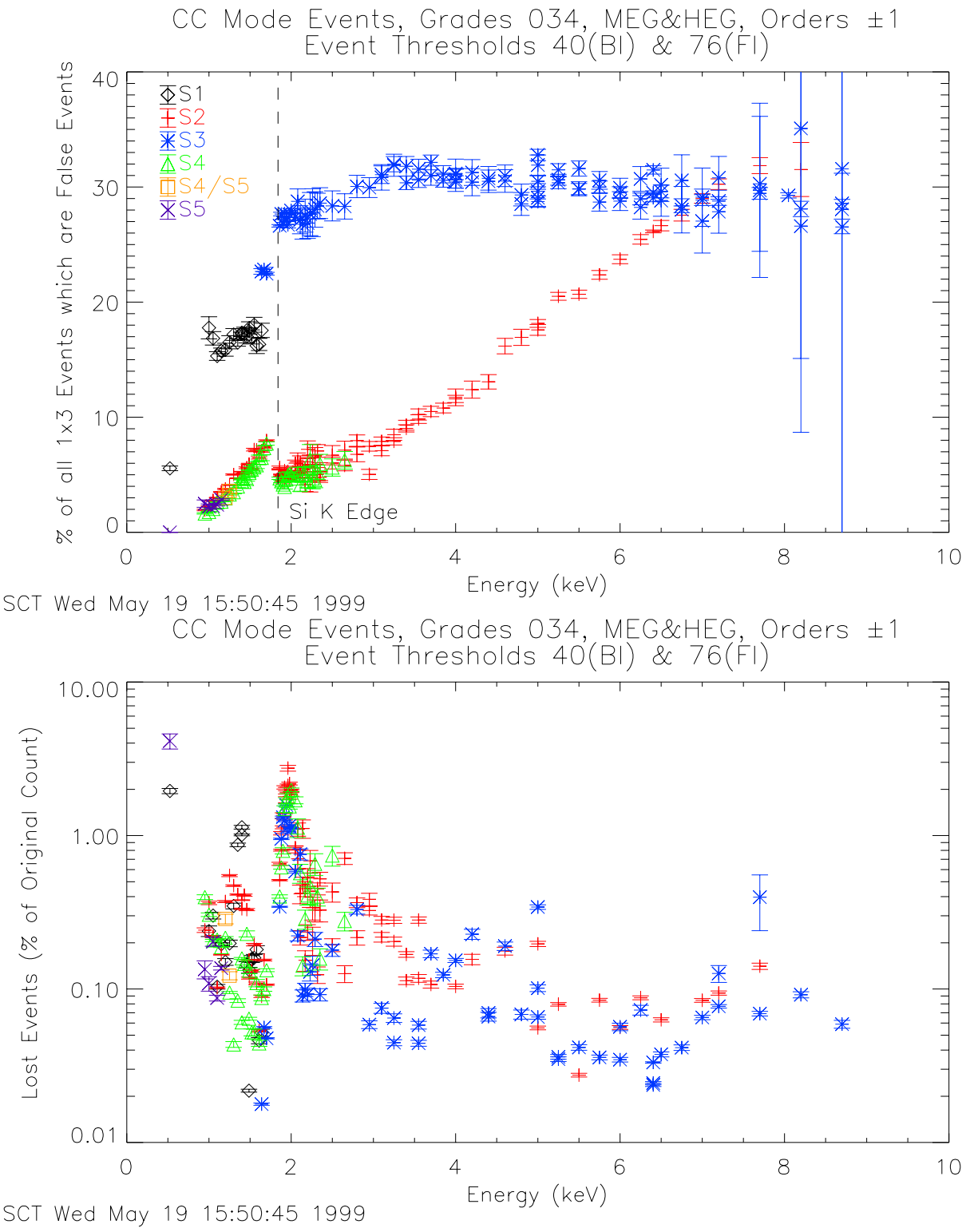

Figure 21. Effect of raising event thresholds on the number of false and actual events. Event thresholds here were doubled to 40 BI and 76 FI to determine if there was an event in the top or bottom rows. The top plot shows percent of CC(1x3) mode events which appeared in the top or bottom row in the TE 3x3 event island, compared to the total CC mode events from all rows. The bottom plot shows the percent of lost actual events resulting from raising these thresholds. The error bar on each point for both plots is the error derived from the statistical uncertainty.

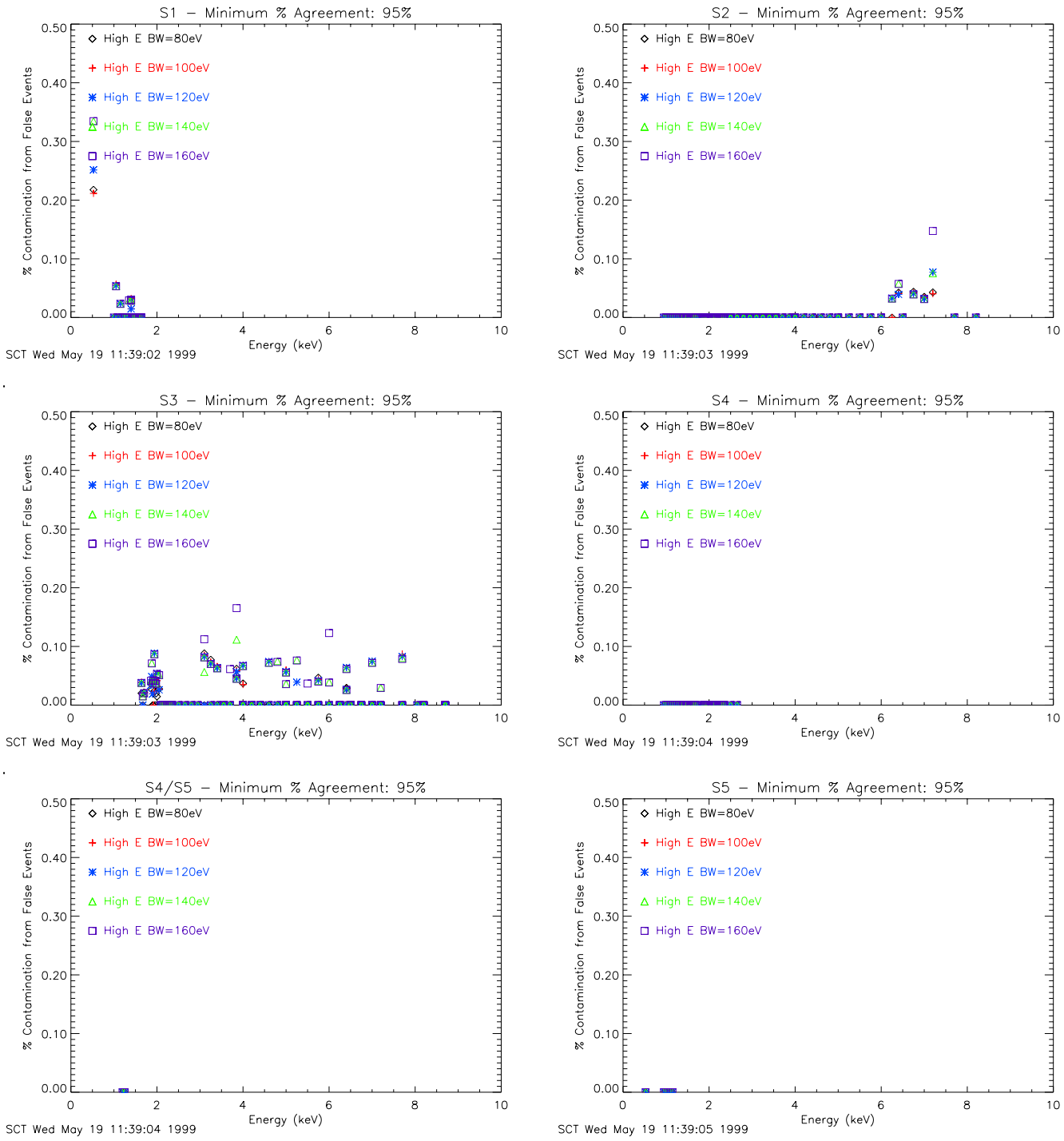

Figure 22. The number of false events included when using the bandwidths shown in Figure 19. There is a different symbol and color used for each upper energy bandwidth; black ◇ for +80 eV, red + for +100 eV, blue ∗ for +120 eV, green △ for +140 eV, and purple □ for +160 eV.

5. CONCLUSIONS

We used XRCF measurements in TE mode, in the energy range of 0.525 to 8.4 keV, to analyze the QE effects when using CC mode. We converted each 3x3 event from the standard ASCA grade set in TE mode to three 1x3 events, using standard event and split thresholds to determine if an event would have been registered. Our analysis resulted in the following conclusions:

- The drop in QE when using CC(1x3) mode compared to TE mode is a maximum of 55% for BI chips (at 3 keV), and 50% for FI chips (at 8 keV). This drop is likely to be greater for FI chips at higher energies.
- There is a strong effect on the QE at the Si-K edge at 1.8 keV. FI and BI chips show opposite behavior when crossing this boundary.
- There is a maximum of 35% false events for BI chips in CC(1x3) mode. this is determined by computing the ratio of the 1x3 events from the top or bottom row of a 3x3 event to all 1x3 events. However, when using CC mode data with a PHA selection about the designated energy with a width determined by 95% of the included TE mode events, the contamination from these false events is less than 0.5%. Therefore, the energies of these events are generally low enough not to be mistaken for actual events.
- The false events have large PHA values, thus changing the event thresholds is not a reasonable way to remove them. By raising the event thresholds for CC(1x3) mode, the percentage of false events is reduced only slightly. This is greatly outweighed by the number of actual events which will be lost, especially at low energies.

6. APPENDIX A

					CC/total at Delta E =				
Chip	Grating	Order	Source	Energy	$\pm 0.08keV$	$\pm 0.10keV$	$\pm 0.12keV$	$\pm 0.14keV$	$\pm 0.16keV$
S1	MEG	-1	O	0.524900	77.9661%	79.1581%	81.1641%	83.5743%	86.1311%
S1	HEG	-1	DCM	1.00000	60.6145%	63.4798%	68.0395%	70.7593%	73.1295%
S1	HEG	-1	DCM	1.05000	73.7918%	73.1393%	72.0379%	73.3813%	74.8858%
S1	HEG	-1	DCM	1.10000	73.5075%	73.0667%	73.5219%	74.3898%	75.9019%
S1	HEG	-1	DCM	1.15000	72.7345%	72.7010%	73.0620%	74.3062%	75.7133%
S1	HEG	-1	DCM	1.20000	66.2145%	68.0088%	70.3626%	72.8344%	75.3306%
S1	HEG	-1	DCM	1.25000	55.4974%	62.3142%	67.3857%	71.0101%	74.1466%
S1	HEG	-1	DCM	1.30000	68.4537%	69.0406%	70.3772%	72.9681%	74.6454%
S1	HEG	-1	DCM	1.35000	71.7019%	71.9757%	73.6477%	74.5131%	75.8074%
S1	HEG	-1	DCM	1.40000	72.9933%	73.0718%	73.8535%	74.6771%	76.2266%
S1	HEG	-1	DCM	1.40000	70.8348%	71.2887%	72.1519%	73.7463%	75.0000%
S1	HEG	-1	DCM	1.43000	72.4696%	73.8994%	73.6187%	74.9637%	75.8604%
S1	HEG	-1	DCM	1.46000	75.3278%	74.8380%	74.3003%	75.3458%	76.5336%
S1	HEG	-1	Al	1.48670	73.0812%	72.9561%	73.6251%	74.2915%	75.4646%
S1	HEG	-1	DCM	1.49000	75.3262%	75.3274%	75.0727%	74.7111%	74.8192%
S1	HEG	-1	DCM	1.52000	72.4696%	73.3574%	74.1157%	75.0677%	76.0106%
S1	HEG	-1	DCM	1.55000	66.4000%	66.5684%	69.3684%	71.4208%	73.6559%
S1	HEG	-1	DCM	1.58000	58.6157%	63.1406%	68.7697%	72.7329%	75.4717%
S1	HEG	-1	DCM	1.61000	49.9456%	58.8586%	66.5553%	71.6635%	75.3717%
S1	HEG	-1	DCM	1.64000	51.4599%	59.0909%	65.3743%	70.3233%	73.5263%

Table 3. Number of CC mode counts within the listed bandwidth about the TE centroid, compared to all of the CC mode counts, for chip S1.

					CC/total at Delta E =				
Chip	Grating	Order	Source	Energy	$\pm 0.08keV$	$\pm 0.10keV$	$\pm 0.12keV$	$\pm 0.14keV$	$\pm 0.16keV$
S2	MEG	-1	DCM	0.950000	93.8571%	94.2574%	94.6347%	95.1408%	95.3554%
S2	MEG	-1	DCM	1.00000	93.9920%	94.3722%	94.9629%	95.4221%	95.8542%
S2	MEG	-1	DCM	1.05000	93.4074%	93.6486%	94.0509%	94.5074%	95.0454%
S2	MEG	-1	DCM	1.10000	93.0718%	93.4373%	93.8040%	94.1021%	94.4432%
S2	MEG	-1	DCM	1.15000	92.4159%	92.7406%	93.2373%	93.7630%	94.1737%
S2	MEG	-1	DCM	1.20000	92.2745%	92.6043%	93.0461%	93.5463%	93.8676%
S2	MEG	-1	DCM	1.25000	91.5868%	92.0187%	92.5342%	93.1278%	93.3932%
S2	MEG	-1	DCM	1.30000	90.1688%	90.6610%	91.1832%	91.6911%	92.0214%
S2	MEG	-1	DCM	1.35000	90.4798%	90.9331%	91.4594%	92.0236%	92.5524%
S2	MEG	-1	DCM	1.40000	90.0933%	90.5171%	90.9372%	91.4429%	91.8491%
S2	MEG	-1	DCM	1.40000	89.9094%	90.3659%	90.8636%	91.4602%	92.0110%
S2	MEG	-1	DCM	1.43000	89.8311%	90.4645%	91.1022%	91.6044%	92.1821%
S2	MEG	-1	DCM	1.46000	89.2338%	89.7419%	90.1882%	90.8011%	91.2430%
S2	MEG	-1	Al	1.48670	88.5136%	89.0866%	89.5964%	90.1630%	90.7396%
S2	MEG	-1	DCM	1.49000	88.6959%	88.9806%	89.4839%	90.0105%	90.4726%
S2	MEG	-1	DCM	1.52000	89.1829%	89.5018%	89.8859%	90.4039%	91.0366%
S2	MEG	-1	DCM	1.55000	86.9146%	87.5396%	88.0671%	88.6547%	89.0877%
S2	MEG	-1	DCM	1.58000	87.3205%	87.7519%	88.3521%	88.7811%	89.3172%
S2	MEG	-1	DCM	1.61000	87.8548%	88.0464%	88.5802%	89.2374%	89.6993%
S2	MEG	-1	DCM	1.64000	86.4218%	87.0137%	87.3818%	88.0646%	88.5187%
S2	MEG	-1	DCM	1.67000	85.5343%	86.0037%	86.7756%	87.4398%	88.2720%
S2	MEG	-1	DCM	1.70000	84.6340%	85.1907%	86.0758%	86.8788%	87.5564%
S2	HEG	-1	DCM	1.86000	90.1142%	90.3234%	90.7573%	91.2077%	91.4475%
S2	MEG	-1	DCM	1.86000	90.4863%	90.6931%	91.1856%	91.6631%	92.0462%
S2	HEG	-1	DCM	1.88000	92.1699%	92.3944%	92.6836%	93.0355%	93.1386%
S2	MEG	-1	DCM	1.88000	91.2496%	91.7169%	91.9942%	92.3793%	92.6568%
S2	HEG	-1	DCM	1.90000	92.0363%	92.6769%	92.9273%	93.0176%	93.4172%
S2	MEG	-1	DCM	1.90000	92.3692%	92.4399%	92.8625%	93.2123%	93.4949%
S2	HEG	-1	DCM	1.92000	91.5089%	91.6136%	91.9916%	92.2794%	92.6586%
S2	MEG	-1	DCM	1.92000	93.1522%	93.2983%	93.4543%	93.5873%	93.7107%
S2	HEG	-1	DCM	1.94000	92.1331%	92.1666%	92.4975%	92.8079%	92.9238%
S2	MEG	-1	DCM	1.94000	91.6596%	91.9328%	92.2046%	92.3433%	92.5815%
S2	HEG	-1	DCM	1.96000	92.0603%	92.5123%	92.8117%	93.0549%	93.2720%
S2	MEG	-1	DCM	1.96000	91.7434%	92.0382%	92.3097%	92.5858%	92.6651%
S2	HEG	-1	DCM	1.98000	92.0863%	92.3688%	92.8228%	93.1590%	93.3913%
S2	MEG	-1	DCM	1.98000	92.1649%	92.4497%	92.6657%	92.8972%	93.3209%
S2	HEG	-1	DCM	2.00000	91.6023%	91.7300%	92.1498%	92.4165%	92.7928%
S2	MEG	-1	DCM	2.00000	91.4894%	91.7667%	91.9821%	92.2456%	92.4705%
S2	HEG	-1	DCM	2.05000	91.2644%	91.7323%	92.1448%	92.4444%	92.4862%
S2	MEG	-1	DCM	2.05000	91.8777%	92.0798%	92.3274%	92.7296%	92.8458%
S2	HEG	-1	DCM	2.08000	92.2956%	92.3664%	92.8463%	93.1818%	92.9110%
S2	MEG	-1	DCM	2.08000	91.1336%	91.3091%	92.1225%	92.7095%	92.7174%
S2	HEG	-1	DCM	2.11000	90.4690%	90.7738%	91.1243%	91.1765%	91.4706%
S2	MEG	-1	DCM	2.11000	90.9976%	90.6760%	91.3395%	91.4747%	91.5235%
S2	HEG	-1	DCM	2.14000	90.7407%	91.0334%	91.1677%	91.7910%	92.2734%
S2	MEG	-1	DCM	2.14000	90.9582%	91.5900%	92.0261%	92.5974%	92.7461%
S2	HEG	-1	DCM	2.17000	92.7835%	93.4454%	94.0496%	94.3987%	94.3987%
S2	MEG	-1	DCM	2.17000	90.5063%	91.1221%	91.3203%	91.5854%	91.9708%
S2	HEG	-1	DCM	2.20000	90.8555%	91.5108%	91.9771%	92.1316%	92.1875%
S2	MEG	-1	DCM	2.20000	89.6104%	89.7077%	90.0253%	90.4282%	91.0916%

Table 4. Number of CC mode counts within the listed bandwidth about the TE centroid, compared to all of the CC mode counts, for chip S2 (part 1).

					CC/total at Delta E =				
Chip	Grating	Order	Source	Energy	$\pm 0.08keV$	$\pm 0.10keV$	$\pm 0.12keV$	$\pm 0.14keV$	$\pm 0.16keV$
S2	HEG	-1	DCM	2.23000	93.2203%	93.9110%	94.1589%	94.1725%	94.4056%
S2	MEG	-1	DCM	2.23000	91.1488%	91.6974%	91.9708%	92.1818%	92.5590%
S2	HEG	-1	DCM	2.26000	90.9910%	90.4656%	90.3084%	91.4097%	91.4286%
S2	MEG	-1	DCM	2.26000	89.9065%	90.0543%	90.4847%	91.2343%	91.6071%
S2	HEG	-1	DCM	2.29000	91.5441%	92.1005%	92.0071%	92.0354%	92.2262%
S2	MEG	-1	DCM	2.29000	91.4566%	91.1805%	91.5094%	91.9571%	92.1123%
S2	HEG	-1	DCM	2.32000	92.1303%	92.1543%	92.5729%	92.8571%	92.9987%
S2	MEG	-1	DCM	2.32000	89.2246%	89.5508%	89.4482%	90.0483%	90.4532%
S2	HEG	-1	DCM	2.35000	92.6199%	92.2939%	92.5267%	92.9329%	93.3216%
S2	MEG	-1	DCM	2.35000	91.8605%	92.4634%	92.8571%	93.0000%	93.3555%
S2	HEG	-1	DCM	2.50000	89.5072%	89.9225%	90.1235%	90.4468%	90.7975%
S2	MEG	-1	DCM	2.50000	90.6149%	90.9375%	91.2461%	91.3758%	91.7864%
S2	HEG	-1	DCM	2.65000	89.2550%	89.3793%	89.7681%	90.2307%	90.5149%
S2	MEG	-1	DCM	2.65000	91.3880%	91.2109%	91.3793%	92.0726%	92.2053%
S2	HEG	-1	DCM	2.80000	89.7041%	90.3559%	90.9297%	91.1964%	91.2063%
S2	MEG	-1	DCM	2.80000	87.9936%	88.4914%	88.8717%	89.1705%	89.5180%
S2	HEG	-1	DCM	2.95000	90.8608%	91.4547%	91.6000%	92.0160%	92.3230%
S2	MEG	-1	DCM	2.95000	90.0572%	89.8270%	90.0409%	90.0748%	90.1695%
S2	HEG	-1	DCM	3.10000	88.8706%	89.5604%	89.6685%	90.0769%	90.4908%
S2	MEG	-1	DCM	3.10000	88.5804%	88.5316%	89.1408%	89.1860%	89.5425%
S2	HEG	-1	DCM	3.25000	87.1525%	87.1720%	87.7331%	87.9004%	88.3523%
S2	MEG	-1	DCM	3.25000	87.7973%	88.1768%	88.3015%	88.7695%	89.1813%
S2	HEG	-1	DCM	3.40000	85.6061%	86.4212%	86.9875%	87.0644%	87.7575%
S2	MEG	-1	DCM	3.40000	87.1700%	87.3614%	87.6316%	88.0454%	88.3377%
S2	HEG	-1	DCM	3.55000	85.4807%	85.7054%	86.1416%	86.7273%	87.1299%
S2	MEG	-1	DCM	3.55000	84.8947%	85.3989%	85.6650%	86.2035%	86.5300%
S2	HEG	-1	DCM	3.70000	85.2401%	85.1789%	85.5314%	85.9756%	86.3082%
S2	HEG	-1	DCM	3.85000	83.5754%	83.7283%	84.2916%	85.0000%	85.3001%
S2	HEG	-1	DCM	4.00000	82.8295%	83.1618%	83.4292%	83.8398%	84.3137%
S2	HEG	-1	DCM	4.00000	82.7957%	82.9146%	83.1829%	83.6868%	84.2405%
S2	HEG	-1	DCM	4.20000	81.8100%	81.6102%	82.0513%	82.1750%	82.8595%
S2	HEG	-1	DCM	4.40000	81.0320%	80.7848%	80.9743%	81.9010%	82.3834%
S2	HEG	-1	DCM	4.60000	75.1026%	75.4464%	76.1846%	76.7132%	77.5424%
S2	HEG	-1	DCM	4.80000	75.2628%	75.5541%	75.8945%	76.5693%	77.2363%
S2	HEG	-1	DCM	5.00000	72.2998%	72.8887%	73.4135%	74.2449%	75.1925%
S2	HEG	-1	DCM	5.00000	72.3545%	72.9365%	73.4453%	74.5349%	75.0506%
S2	HEG	-1	DCM	5.25000	70.0608%	70.7115%	70.8749%	71.4326%	72.1498%
S2	HEG	-1	DCM	5.50000	69.1868%	69.3280%	69.8403%	70.7261%	71.3061%
S2	HEG	-1	DCM	5.75000	65.8241%	66.1367%	66.8183%	67.9178%	68.9604%
S2	HEG	-1	DCM	6.00000	64.2225%	65.1978%	65.7231%	66.0763%	66.9733%
S2	HEG	-1	DCM	6.25000	60.2102%	60.8725%	61.9632%	62.8733%	63.8258%
S2	HEG	-1	Fe	6.40380	58.8581%	59.2381%	60.0738%	60.8145%	61.2820%
S2	HEG	-1	DCM	6.50000	59.0137%	59.8650%	59.8164%	60.4921%	61.0512%
S2	HEG	-1	DCM	6.75000	57.8501%	58.1964%	59.3512%	59.7683%	60.0530%
S2	HEG	-1	DCM	7.00000	54.7213%	54.7003%	55.6196%	55.9014%	56.7976%
S2	HEG	-1	DCM	7.20000	57.5587%	57.9302%	58.2622%	58.4815%	58.4527%
S2	HEG	-1	DCM	7.70000	54.9708%	54.7511%	54.6643%	55.4237%	56.2020%
S2	HEG	-1	DCM	8.20000	51.4151%	51.7241%	51.4620%	52.5830%	53.2258%

Table 5. Number of CC mode counts within the listed bandwidth about the TE centroid, compared to all of the CC mode counts, for chip S2 (part 2).

					CC/total at Delta E =				
Chip	Grating	Order	Source	Energy	$\pm 0.08keV$	$\pm 0.10keV$	$\pm 0.12keV$	$\pm 0.14keV$	$\pm 0.16keV$
S3	MEG	1	DCM	1.64000	62.8583%	63.2503%	64.4737%	66.0885%	67.7031%
S3	MEG	1	DCM	1.67000	63.0979%	63.7549%	64.7307%	66.0661%	67.4524%
S3	MEG	1	DCM	1.70000	64.2476%	64.8905%	65.5581%	66.8907%	68.4649%
S3	MEG	1	DCM	1.86000	55.7380%	56.4710%	57.4588%	58.9710%	60.4396%
S3	MEG	1	DCM	1.88000	54.2184%	54.8750%	55.4258%	57.0435%	58.5369%
S3	MEG	1	DCM	1.90000	54.3135%	54.8571%	56.1154%	57.5027%	59.3947%
S3	MEG	1	DCM	1.92000	52.9211%	53.6321%	54.6392%	56.2077%	57.8543%
S3	MEG	1	DCM	1.94000	54.3248%	55.0802%	56.1515%	57.2764%	59.0871%
S3	MEG	1	DCM	1.96000	54.0111%	54.9672%	56.1578%	57.7724%	59.0311%
S3	MEG	1	DCM	1.98000	52.4958%	53.3257%	54.8756%	56.4548%	58.2648%
S3	MEG	1	DCM	2.00000	53.2742%	53.9603%	54.9221%	56.2184%	57.5983%
S3	MEG	1	DCM	2.05000	51.6880%	52.8785%	54.8321%	56.2671%	57.8598%
S3	MEG	1	DCM	2.08000	49.0446%	50.1672%	51.5898%	54.1048%	55.3159%
S3	MEG	1	DCM	2.11000	52.3810%	53.0864%	53.8182%	55.4862%	56.8662%
S3	MEG	1	DCM	2.14000	52.3026%	53.4205%	55.4695%	57.5758%	58.7302%
S3	MEG	1	DCM	2.17000	51.6364%	52.5785%	54.4480%	56.2698%	57.3805%
S3	MEG	1	DCM	2.20000	51.6903%	53.5168%	56.0591%	57.3230%	59.3660%
S3	MEG	1	DCM	2.23000	51.6820%	52.0626%	53.9638%	56.9672%	58.6345%
S3	MEG	1	DCM	2.26000	49.3716%	51.2397%	52.2692%	54.0832%	56.4885%
S3	MEG	1	DCM	2.29000	51.4916%	52.9904%	54.2857%	55.8036%	57.3481%
S3	MEG	1	DCM	2.32000	51.3011%	51.3169%	52.2204%	54.0693%	55.6175%
S3	MEG	1	DCM	2.35000	47.3398%	48.5830%	50.7812%	53.0318%	55.0476%
S3	MEG	1	DCM	2.50000	50.5285%	52.0710%	53.8241%	54.8780%	55.7924%
S3	MEG	1	DCM	2.65000	49.9555%	52.1268%	53.9019%	55.6171%	57.2214%
S3	MEG	1	DCM	2.80000	46.6081%	48.1645%	49.9645%	51.3570%	53.1444%
S3	MEG	1	DCM	2.95000	47.9720%	48.8179%	50.9938%	52.9664%	54.4465%
S3	HEG	1	DCM	3.10000	46.4880%	48.2612%	49.8379%	50.7109%	52.3922%
S3	MEG	1	DCM	3.10000	47.4716%	48.3778%	49.4457%	50.8724%	52.4272%
S3	HEG	1	DCM	3.25000	47.0167%	47.9622%	48.5080%	49.3869%	50.4730%
S3	MEG	1	DCM	3.25000	45.4250%	46.1384%	47.2050%	49.0104%	50.2793%
S3	HEG	1	DCM	3.40000	45.7554%	47.3062%	48.0697%	49.7878%	51.7158%
S3	MEG	1	DCM	3.40000	48.6328%	49.4144%	49.9354%	51.7518%	53.2278%
S3	HEG	1	DCM	3.55000	46.2203%	47.1513%	47.8207%	49.6368%	50.5995%
S3	MEG	1	DCM	3.55000	46.5649%	47.9479%	49.1734%	50.7878%	52.2477%
S3	HEG	1	DCM	3.70000	49.1673%	50.1639%	51.0533%	51.7633%	53.5062%
S3	MEG	1	DCM	3.70000	47.1739%	47.3606%	48.1238%	49.0626%	50.3827%
S3	HEG	1	DCM	3.85000	51.3478%	51.1559%	51.5118%	52.3060%	53.8584%
S3	MEG	1	DCM	3.85000	48.7328%	49.0038%	50.7409%	52.2727%	53.7532%
S3	HEG	1	DCM	4.00000	50.2150%	51.7346%	51.9695%	53.1128%	54.2431%
S3	HEG	1	DCM	4.00000	49.6158%	50.4425%	50.9242%	52.6553%	54.0998%
S3	MEG	1	DCM	4.00000	48.2157%	48.7071%	49.8997%	51.3470%	52.6958%
S3	MEG	1	DCM	4.00000	47.7016%	49.7242%	50.8160%	51.9509%	53.2338%
S3	HEG	1	DCM	4.20000	52.9101%	52.6415%	53.1500%	54.0913%	55.2921%
S3	MEG	1	DCM	4.20000	46.8687%	47.6965%	48.6441%	49.6716%	50.4831%
S3	HEG	1	DCM	4.40000	53.1429%	52.6936%	53.0660%	53.3988%	54.1543%
S3	MEG	1	DCM	4.40000	51.3351%	50.8867%	51.0160%	51.7945%	53.1900%
S3	HEG	1	DCM	4.60000	53.3333%	53.7867%	54.3924%	54.8159%	55.9275%
S3	MEG	1	DCM	4.60000	47.2222%	48.5736%	51.1001%	52.8562%	53.6486%
S3	HEG	1	DCM	4.80000	54.2597%	55.1543%	55.8074%	56.4979%	57.8451%
S3	MEG	1	DCM	4.80000	56.3080%	56.6584%	56.0338%	57.2909%	58.2973%

Table 6. Number of CC mode counts within the listed bandwidth about the TE centroid, compared to all of the CC mode counts, for chip S3 (part 1).

					CC/total at Delta E =				
Chip	Grating	Order	Source	Energy	$\pm 0.08keV$	$\pm 0.10keV$	$\pm 0.12keV$	$\pm 0.14keV$	$\pm 0.16keV$
S3	HEG	1	DCM	5.00000	53.9239%	53.9946%	53.9619%	55.2311%	55.7354%
S3	HEG	1	DCM	5.00000	56.5937%	56.2278%	56.2386%	57.0873%	58.1837%
S3	MEG	-1	DCM	5.00000	46.4655%	46.2614%	47.3650%	49.2772%	51.2361%
S3	MEG	-1	DCM	5.00000	44.9647%	45.9036%	47.1256%	48.1953%	49.9479%
S3	MEG	1	DCM	5.00000	54.2043%	54.3838%	55.2813%	56.2327%	57.5708%
S3	MEG	1	DCM	5.00000	52.3743%	53.5759%	54.5384%	56.0793%	57.0956%
S3	HEG	1	DCM	5.25000	54.5700%	55.7769%	56.2106%	57.3870%	57.8343%
S3	MEG	-1	DCM	5.25000	46.5027%	47.1422%	48.6161%	50.3873%	51.8040%
S3	MEG	1	DCM	5.25000	51.3539%	52.3532%	53.3931%	54.5796%	55.5637%
S3	HEG	1	DCM	5.50000	57.7194%	56.8144%	57.3129%	58.4497%	58.7290%
S3	MEG	-1	DCM	5.50000	47.5077%	47.7580%	48.0461%	49.7121%	51.1715%
S3	MEG	1	DCM	5.50000	54.2297%	55.1010%	54.9554%	56.1404%	57.1679%
S3	HEG	1	DCM	5.75000	58.4608%	58.3296%	58.1864%	58.5415%	58.6086%
S3	MEG	-1	DCM	5.75000	49.6124%	51.1236%	52.2807%	53.5614%	54.8051%
S3	MEG	1	DCM	5.75000	57.5130%	58.0878%	58.3131%	58.7182%	59.5925%
S3	HEG	1	DCM	6.00000	56.6122%	57.0933%	57.5806%	57.8907%	58.8081%
S3	MEG	-1	DCM	6.00000	48.3372%	50.5450%	52.0913%	53.4398%	54.5183%
S3	MEG	1	DCM	6.00000	56.9145%	57.2541%	57.8710%	58.5591%	59.4611%
S3	HEG	1	DCM	6.25000	61.3015%	59.8865%	60.7042%	61.0982%	61.1467%
S3	MEG	-1	DCM	6.25000	48.5236%	49.4746%	51.5841%	53.3333%	54.1699%
S3	MEG	1	DCM	6.25000	57.7713%	59.1537%	58.2803%	58.8593%	59.6726%
S3	HEG	1	Fe	6.40380	58.3489%	58.5155%	58.8662%	59.2318%	59.8636%
S3	MEG	-1	Fe	6.40380	49.0226%	50.0000%	50.7177%	52.1049%	52.8832%
S3	MEG	1	Fe	6.40380	60.3933%	59.8267%	58.5242%	58.7703%	58.8252%
S3	HEG	1	DCM	6.50000	53.9432%	55.7362%	56.5330%	57.7769%	58.6332%
S3	MEG	-1	DCM	6.50000	48.2353%	49.4145%	51.4317%	52.5817%	53.9256%
S3	MEG	1	DCM	6.50000	58.7131%	59.2152%	58.5209%	59.4262%	60.1796%
S3	HEG	1	DCM	6.75000	54.3608%	56.4331%	58.0879%	58.9885%	60.0447%
S3	MEG	-1	DCM	6.75000	51.1952%	53.9711%	54.2429%	54.1534%	55.3991%
S3	MEG	1	DCM	6.75000	59.7917%	56.8100%	57.7303%	58.7963%	60.0000%
S3	HEG	1	DCM	7.00000	55.6273%	57.0726%	57.4436%	58.6021%	59.2942%
S3	MEG	-1	DCM	7.00000	52.2782%	52.3711%	53.4884%	55.7009%	57.1429%
S3	MEG	1	DCM	7.00000	62.0787%	62.8079%	60.8791%	61.6352%	61.9433%
S3	HEG	1	DCM	7.20000	60.1695%	60.3755%	60.3390%	61.2203%	62.2685%
S3	MEG	-1	DCM	7.20000	49.6441%	51.1485%	52.2111%	52.3098%	53.9894%
S3	MEG	1	DCM	7.20000	58.1749%	59.5601%	57.7099%	59.7701%	59.9721%
S3	HEG	1	DCM	7.70000	58.8608%	59.3764%	60.7052%	61.5508%	61.8919%
S3	MEG	-1	DCM	7.70000	51.4286%	51.7413%	57.0093%	55.8036%	55.9829%
S3	MEG	1	DCM	7.70000	57.7236%	59.0278%	57.0552%	58.2353%	56.8182%
S3	HEG	1	Cu	8.04780	60.3494%	60.8808%	61.0519%	62.2765%	63.0561%
S3	HEG	1	DCM	8.20000	56.3852%	58.3995%	58.8300%	59.0790%	60.0602%
S3	MEG	-1	DCM	8.20000	36.0000%	36.3636%	39.3443%	36.9231%	41.5385%
S3	MEG	1	DCM	8.20000	56.6038%	60.0000%	60.0000%	55.7143%	54.0541%
S3	HEG	-1	DCM	8.70000	54.1311%	58.2927%	59.8670%	63.2353%	63.1791%
S3	HEG	1	DCM	8.70000	58.5411%	58.3861%	57.8270%	59.2266%	60.1568%
S3	MEG	-1	DCM	8.70000	44.8276%	51.7241%	57.5758%	54.2857%	60.0000%
S3	MEG	1	DCM	8.70000	51.8519%	58.6207%	54.5455%	57.1429%	57.1429%

Table 7. Number of CC mode counts within the listed bandwidth about the TE centroid, compared to all of the CC mode counts, for chip S3 (part 2).

					CC/total at Delta E =				
Chip	Grating	Order	Source	Energy	$\pm 0.08keV$	$\pm 0.10keV$	$\pm 0.12keV$	$\pm 0.14keV$	$\pm 0.16keV$
S4	MEG	1	DCM	0.950000	93.4408%	93.7685%	94.2109%	94.5221%	95.2259%
S4	MEG	1	DCM	1.00000	93.1883%	93.8596%	94.3896%	94.9592%	95.3279%
S4	MEG	1	DCM	1.05000	93.3381%	93.7577%	94.0566%	94.4162%	94.8116%
S4	MEG	1	DCM	1.10000	92.6028%	93.0468%	93.3626%	93.8626%	94.2742%
S4	MEG	1	DCM	1.15000	92.3388%	92.7308%	93.0973%	93.5580%	93.9566%
S4	MEG	1	DCM	1.20000	92.2760%	92.6223%	92.9250%	93.6145%	93.8441%
S4	MEG	1	DCM	1.25000	91.9555%	92.3214%	92.7443%	93.3011%	93.8536%
S4	HEG	1	DCM	1.30000	91.0348%	91.5743%	91.9398%	92.5353%	93.1567%
S4	HEG	1	DCM	1.35000	90.8986%	91.4269%	92.0978%	92.5021%	92.8794%
S4	HEG	1	DCM	1.40000	89.8561%	90.2082%	90.6890%	91.1191%	91.7267%
S4	HEG	1	DCM	1.40000	89.3617%	89.9598%	90.6404%	91.2469%	91.7510%
S4	HEG	1	DCM	1.43000	89.5980%	90.0248%	90.4550%	91.0617%	91.4652%
S4	HEG	1	DCM	1.46000	90.0706%	90.3918%	90.7528%	91.1874%	91.7478%
S4	HEG	1	Al	1.48670	88.9502%	89.4302%	90.0173%	90.4690%	90.7168%
S4	HEG	1	DCM	1.49000	87.9021%	88.6404%	89.1604%	89.5390%	90.3412%
S4	HEG	1	DCM	1.52000	87.5269%	87.8981%	88.8537%	89.2819%	89.7098%
S4	HEG	1	DCM	1.55000	87.8998%	88.5021%	89.0289%	89.5068%	89.7906%
S4	HEG	1	DCM	1.58000	87.7815%	88.2582%	88.7410%	89.2758%	89.6247%
S4	HEG	1	DCM	1.61000	86.2700%	86.6697%	87.4441%	87.9964%	88.6759%
S4	HEG	1	DCM	1.64000	88.0218%	88.4564%	88.5727%	89.0368%	89.6277%
S4	HEG	1	DCM	1.67000	84.5325%	84.9693%	85.6563%	86.5002%	87.0957%
S4	HEG	1	DCM	1.70000	85.6082%	85.6495%	86.0167%	86.4422%	86.8757%
S4	HEG	1	DCM	1.86000	90.8094%	90.9981%	91.3590%	91.8481%	92.2304%
S4	HEG	1	DCM	1.88000	91.8636%	92.2245%	92.6914%	92.8798%	92.9699%
S4	HEG	1	DCM	1.90000	92.2513%	92.1819%	92.3737%	92.9110%	93.1206%
S4	HEG	1	DCM	1.92000	92.3256%	92.6678%	92.7731%	93.0401%	93.2815%
S4	HEG	1	DCM	1.94000	91.8196%	92.0267%	92.3038%	92.6284%	92.8571%
S4	HEG	1	DCM	1.96000	91.7867%	92.1875%	92.3472%	92.7514%	92.6829%
S4	HEG	1	DCM	1.98000	91.0632%	91.2360%	91.6889%	91.9134%	92.2874%
S4	HEG	1	DCM	2.00000	91.3933%	91.6534%	91.6327%	91.9813%	92.2502%
S4	HEG	1	DCM	2.05000	91.1713%	91.6330%	92.1053%	92.4743%	92.7231%
S4	HEG	1	DCM	2.08000	92.0437%	92.5419%	92.9110%	93.0827%	93.1138%
S4	HEG	1	DCM	2.11000	92.3930%	92.7245%	93.1087%	93.5780%	93.4551%
S4	HEG	1	DCM	2.14000	91.1003%	91.0970%	91.6404%	91.8750%	92.2481%
S4	HEG	1	DCM	2.17000	92.1630%	92.0000%	92.3313%	92.7914%	92.5419%
S4	HEG	1	DCM	2.20000	92.6154%	93.2432%	93.3530%	93.4018%	93.4114%
S4	HEG	1	DCM	2.23000	91.1168%	91.3793%	91.6870%	91.4634%	91.4634%
S4	HEG	1	DCM	2.26000	89.6714%	90.6179%	90.8467%	91.5525%	91.5525%
S4	HEG	1	DCM	2.29000	91.4657%	91.5771%	91.5044%	91.8871%	92.0775%
S4	HEG	1	DCM	2.32000	92.2619%	92.4964%	92.6829%	92.4394%	92.5820%
S4	HEG	1	DCM	2.35000	89.4921%	90.0855%	90.6143%	90.8007%	90.6937%
S4	HEG	1	DCM	2.50000	90.8027%	91.5171%	91.8006%	92.1474%	92.1974%
S4	HEG	1	DCM	2.65000	90.3937%	90.2549%	90.1639%	90.8419%	90.8689%

Table 8. Number of CC mode counts within the listed bandwidth about the TE centroid, compared to all of the CC mode counts, for chip S4.

					CC/total at Delta E =				
Chip	Grating	Order	Source	Energy	$\pm 0.08keV$	$\pm 0.10keV$	$\pm 0.12keV$	$\pm 0.14keV$	$\pm 0.16keV$
S4/S5	HEG	1	DCM	1.20000	92.4779%	92.9773%	93.7318%	93.8998%	94.4162%
S4/S5	HEG	1	DCM	1.25000	91.9975%	92.3655%	92.6342%	92.8304%	93.1507%

Table 9. Number of CC mode counts within the listed bandwidth about the TE centroid, compared to all of the CC mode counts, for lines spanning the gap between chips S4 and S5.

					CC/total at Delta E =				
Chip	Grating	Order	Source	Energy	$\pm 0.08keV$	$\pm 0.10keV$	$\pm 0.12keV$	$\pm 0.14keV$	$\pm 0.16keV$
S5	MEG	1	O	0.524900	94.9383%	95.8384%	96.4634%	96.5937%	97.4515%
S5	HEG	1	DCM	0.950000	94.1259%	94.1667%	94.4751%	94.7586%	94.7658%
S5	HEG	1	DCM	1.00000	92.4972%	93.0078%	93.5982%	93.9294%	94.1501%
S5	HEG	1	DCM	1.05000	93.9394%	94.1917%	94.5720%	94.9270%	95.2183%
S5	HEG	1	DCM	1.10000	93.0631%	93.4938%	93.7278%	94.1333%	94.6785%
S5	HEG	1	DCM	1.15000	93.1576%	93.4892%	93.7621%	94.1860%	94.5781%

Table 10. Number of CC mode counts within the listed bandwidth about the TE centroid, compared to all of the CC mode counts, for chip S5.

7. APPENDIX B

					Low Energy Limit for High Energy Limit =				
Chip	Grating	Order	Source	Energy	$0.08keV$	$0.10keV$	$0.12keV$	$0.14keV$	$0.16keV$
S1	MEG	-1	O	0.524900	0.253	0.278	0.304	0.311	0.311
S1	HEG	-1	DCM	1.00000	0.399	0.456	0.500	0.551	0.566
S1	HEG	-1	DCM	1.05000	0.369	0.434	0.497	0.525	0.554
S1	HEG	-1	DCM	1.10000	0.433	0.478	0.513	0.538	0.559
S1	HEG	-1	DCM	1.15000	0.392	0.478	0.540	0.572	0.592
S1	HEG	-1	DCM	1.20000	0.437	0.551	0.604	0.656	0.673
S1	HEG	-1	DCM	1.25000	0.494	0.588	0.646	0.684	0.692
S1	HEG	-1	DCM	1.30000	0.408	0.532	0.625	0.666	0.706
S1	HEG	-1	DCM	1.35000	0.423	0.533	0.610	0.647	0.674
S1	HEG	-1	DCM	1.40000	0.449	0.550	0.610	0.658	0.681
S1	HEG	-1	DCM	1.40000	0.488	0.600	0.649	0.677	0.703
S1	HEG	-1	DCM	1.43000	0.467	0.562	0.635	0.674	0.704
S1	HEG	-1	DCM	1.46000	0.435	0.567	0.662	0.706	0.734
S1	HEG	-1	Al	1.48670	0.431	0.570	0.648	0.704	0.744
S1	HEG	-1	DCM	1.49000	0.403	0.523	0.625	0.689	0.745
S1	HEG	-1	DCM	1.52000	0.407	0.553	0.652	0.715	0.779
S1	HEG	-1	DCM	1.55000	0.518	0.693	0.759	0.793	0.819
S1	HEG	-1	DCM	1.58000	0.509	0.682	0.767	0.810	0.844
S1	HEG	-1	DCM	1.61000	0.607	0.748	0.816	0.847	0.863
S1	HEG	-1	DCM	1.64000	0.616	0.760	0.845	0.871	0.893

Table 11. Low energy bandwidth size for extracting the equal number of counts, for chip S1.

					Low Energy Limit for High Energy Limit =				
Chip	Grating	Order	Source	Energy	$0.08keV$	$0.10keV$	$0.12keV$	$0.14keV$	$0.16keV$
S2	MEG	-1	DCM	0.950000	0.528	0.528	0.528	0.528	0.528
S2	MEG	-1	DCM	1.00000	0.508	0.508	0.508	0.508	0.508
S2	MEG	-1	DCM	1.05000	0.615	0.615	0.615	0.615	0.615
S2	MEG	-1	DCM	1.10000	0.598	0.598	0.598	0.598	0.631
S2	MEG	-1	DCM	1.15000	0.639	0.639	0.651	0.651	0.656
S2	MEG	-1	DCM	1.20000	0.616	0.616	0.616	0.616	0.616
S2	MEG	-1	DCM	1.25000	0.640	0.648	0.656	0.656	0.656
S2	MEG	-1	DCM	1.30000	0.659	0.666	0.666	0.666	0.666
S2	MEG	-1	DCM	1.35000	0.667	0.674	0.675	0.690	0.690
S2	MEG	-1	DCM	1.40000	0.687	0.689	0.692	0.694	0.694
S2	MEG	-1	DCM	1.40000	0.688	0.691	0.695	0.695	0.699
S2	MEG	-1	DCM	1.43000	0.725	0.728	0.732	0.732	0.732
S2	MEG	-1	DCM	1.46000	0.745	0.789	0.822	0.822	0.830
S2	MEG	-1	Al	1.48670	0.730	0.739	0.755	0.807	0.807
S2	MEG	-1	DCM	1.49000	0.727	0.731	0.731	0.731	0.732
S2	MEG	-1	DCM	1.52000	0.762	0.771	0.771	0.781	0.781
S2	MEG	-1	DCM	1.55000	0.772	0.775	0.779	0.780	0.780
S2	MEG	-1	DCM	1.58000	0.791	0.806	0.817	0.817	0.817
S2	MEG	-1	DCM	1.61000	0.792	0.804	0.811	0.811	0.814
S2	MEG	-1	DCM	1.64000	0.820	0.820	0.836	0.836	0.836
S2	MEG	-1	DCM	1.67000	0.833	0.840	0.840	0.848	0.848
S2	MEG	-1	DCM	1.70000	0.833	0.840	0.841	0.844	0.844
S2	HEG	-1	DCM	1.86000	0.919	0.942	0.956	0.956	0.964
S2	MEG	-1	DCM	1.86000	0.888	0.895	0.900	0.907	0.907
S2	HEG	-1	DCM	1.88000	0.915	0.950	0.951	0.955	0.955
S2	MEG	-1	DCM	1.88000	0.908	0.914	0.919	0.922	0.926
S2	HEG	-1	DCM	1.90000	0.994	1.00	1.00	1.00	1.00
S2	MEG	-1	DCM	1.90000	1.02	1.18	1.18	1.18	1.18
S2	HEG	-1	DCM	1.92000	0.944	0.944	0.944	0.944	1.03
S2	MEG	-1	DCM	1.92000	0.932	0.937	0.939	0.939	0.939
S2	HEG	-1	DCM	1.94000	0.977	0.977	0.977	0.977	0.977
S2	MEG	-1	DCM	1.94000	0.936	0.936	0.936	0.940	0.946
S2	HEG	-1	DCM	1.96000	0.971	0.971	0.971	0.971	0.978
S2	MEG	-1	DCM	1.96000	0.971	0.977	0.986	0.997	1.00
S2	HEG	-1	DCM	1.98000	0.956	0.974	0.974	0.974	0.974
S2	MEG	-1	DCM	1.98000	0.990	1.00	1.00	1.00	1.00
S2	HEG	-1	DCM	2.00000	0.958	0.984	0.996	0.996	1.00
S2	MEG	-1	DCM	2.00000	0.954	0.963	0.971	0.971	0.971
S2	HEG	-1	DCM	2.05000	0.909	0.912	0.964	0.964	0.964
S2	MEG	-1	DCM	2.05000	1.02	1.02	1.02	1.02	1.02
S2	HEG	-1	DCM	2.08000	1.13	1.13	1.13	1.13	1.13
S2	MEG	-1	DCM	2.08000	1.08	1.18	1.18	1.18	1.18
S2	HEG	-1	DCM	2.11000	1.06	1.06	1.06	1.06	1.06
S2	MEG	-1	DCM	2.11000	1.00	1.00	1.03	1.03	1.03
S2	HEG	-1	DCM	2.14000	1.17	1.17	1.17	1.17	1.17
S2	MEG	-1	DCM	2.14000	1.19	1.19	1.19	1.19	1.19
S2	HEG	-1	DCM	2.17000	1.03	1.03	1.03	1.03	1.03
S2	MEG	-1	DCM	2.17000	1.05	1.05	1.05	1.05	1.05
S2	HEG	-1	DCM	2.20000	1.25	1.25	1.25	1.25	1.25
S2	MEG	-1	DCM	2.20000	1.00	1.00	1.00	1.00	1.00

Table 12. Low energy bandwidth size for extracting the equal number of counts, for chip S2 (part 1).

					Low Energy Limit for High Energy Limit =				
Chip	Grating	Order	Source	Energy	$0.08keV$	$0.10keV$	$0.12keV$	$0.14keV$	$0.16keV$
S2	HEG	-1	DCM	2.23000	1.11	1.11	1.11	1.11	1.11
S2	MEG	-1	DCM	2.23000	1.17	1.17	1.17	1.17	1.17
S2	HEG	-1	DCM	2.26000	0.950	1.03	1.03	1.03	1.03
S2	MEG	-1	DCM	2.26000	1.07	1.07	1.07	1.07	1.07
S2	HEG	-1	DCM	2.29000	1.10	1.10	1.14	1.14	1.14
S2	MEG	-1	DCM	2.29000	1.10	1.13	1.13	1.13	1.13
S2	HEG	-1	DCM	2.32000	1.09	1.20	1.20	1.20	1.20
S2	MEG	-1	DCM	2.32000	1.18	1.37	1.37	1.37	1.37
S2	HEG	-1	DCM	2.35000	1.13	1.13	1.13	1.13	1.13
S2	MEG	-1	DCM	2.35000	1.32	1.32	1.32	1.32	1.32
S2	HEG	-1	DCM	2.50000	1.27	1.27	1.27	1.27	1.27
S2	MEG	-1	DCM	2.50000	1.18	1.22	1.42	1.42	1.42
S2	HEG	-1	DCM	2.65000	1.34	1.48	1.48	1.48	1.48
S2	MEG	-1	DCM	2.65000	1.16	1.20	1.26	1.26	1.28
S2	HEG	-1	DCM	2.80000	1.55	1.55	1.55	1.55	1.55
S2	MEG	-1	DCM	2.80000	1.34	1.44	1.54	1.54	1.54
S2	HEG	-1	DCM	2.95000	1.44	1.45	1.51	1.51	1.51
S2	MEG	-1	DCM	2.95000	1.42	1.48	1.48	1.48	1.48
S2	HEG	-1	DCM	3.10000	1.49	1.52	1.54	1.54	1.54
S2	MEG	-1	DCM	3.10000	1.43	1.43	1.45	1.45	1.45
S2	HEG	-1	DCM	3.25000	1.60	1.61	1.91	1.91	1.97
S2	MEG	-1	DCM	3.25000	1.57	1.60	1.69	1.69	1.69
S2	HEG	-1	DCM	3.40000	1.66	1.67	1.71	1.71	1.71
S2	MEG	-1	DCM	3.40000	1.66	1.68	1.69	1.69	1.69
S2	HEG	-1	DCM	3.55000	1.71	1.75	1.75	1.75	1.75
S2	MEG	-1	DCM	3.55000	1.67	1.74	1.78	1.88	1.88
S2	HEG	-1	DCM	3.70000	1.79	1.83	1.83	1.83	1.83
S2	HEG	-1	DCM	3.85000	1.85	1.91	1.92	1.92	1.92
S2	HEG	-1	DCM	4.00000	1.87	1.94	1.95	1.95	1.96
S2	HEG	-1	DCM	4.00000	1.83	1.97	1.97	1.97	1.98
S2	HEG	-1	DCM	4.20000	1.92	2.02	2.02	2.07	2.07
S2	HEG	-1	DCM	4.40000	2.02	2.11	2.12	2.12	2.15
S2	HEG	-1	DCM	4.60000	2.08	2.12	2.16	2.18	2.17
S2	HEG	-1	DCM	4.80000	2.23	2.33	2.36	2.38	2.38
S2	HEG	-1	DCM	5.00000	2.19	2.32	2.42	2.44	2.45
S2	HEG	-1	DCM	5.00000	2.09	2.24	2.30	2.33	2.34
S2	HEG	-1	DCM	5.25000	2.16	2.30	2.38	2.39	2.41
S2	HEG	-1	DCM	5.50000	2.22	2.40	2.48	2.50	2.53
S2	HEG	-1	DCM	5.75000	2.28	2.46	2.57	2.60	2.62
S2	HEG	-1	DCM	6.00000	2.24	2.42	2.55	2.58	2.61
S2	HEG	-1	DCM	6.25000	2.46	2.59	2.71	2.75	2.77
S2	HEG	-1	Fe	6.40380	2.39	2.56	2.67	2.75	2.81
S2	HEG	-1	DCM	6.50000	2.27	2.51	2.68	2.79	2.86
S2	HEG	-1	DCM	6.75000	2.36	2.60	2.70	2.77	2.86
S2	HEG	-1	DCM	7.00000	2.59	2.79	2.92	3.03	3.08
S2	HEG	-1	DCM	7.20000	2.08	2.26	2.45	2.54	2.63
S2	HEG	-1	DCM	7.70000	2.11	2.32	2.51	2.69	2.80
S2	HEG	-1	DCM	8.20000	2.28	2.42	2.88	3.00	3.16

Table 13. Low energy bandwidth size for extracting the equal number of counts, for chip S2 (part 2).

					Low Energy Limit for High Energy Limit =				
Chip	Grating	Order	Source	Energy	$0.08keV$	$0.10keV$	$0.12keV$	$0.14keV$	$0.16keV$
S3	MEG	1	DCM	1.64000	0.675	0.753	0.792	0.820	0.833
S3	MEG	1	DCM	1.67000	0.666	0.749	0.798	0.825	0.842
S3	MEG	1	DCM	1.70000	0.697	0.763	0.810	0.832	0.846
S3	MEG	1	DCM	1.86000	0.726	0.803	0.851	0.876	0.896
S3	MEG	1	DCM	1.88000	0.717	0.801	0.867	0.894	0.908
S3	MEG	1	DCM	1.90000	0.768	0.849	0.904	0.929	0.947
S3	MEG	1	DCM	1.92000	0.783	0.857	0.906	0.933	0.946
S3	MEG	1	DCM	1.94000	0.757	0.834	0.904	0.936	0.949
S3	MEG	1	DCM	1.96000	0.782	0.867	0.917	0.950	0.969
S3	MEG	1	DCM	1.98000	0.786	0.865	0.913	0.942	0.962
S3	MEG	1	DCM	2.00000	0.814	0.882	0.937	0.967	0.980
S3	MEG	1	DCM	2.05000	0.863	0.931	0.971	1.00	1.01
S3	MEG	1	DCM	2.08000	0.863	0.934	0.998	1.01	1.02
S3	MEG	1	DCM	2.11000	0.880	0.953	1.02	1.02	1.12
S3	MEG	1	DCM	2.14000	0.880	0.983	1.01	1.03	1.06
S3	MEG	1	DCM	2.17000	0.891	0.973	1.01	1.06	1.09
S3	MEG	1	DCM	2.20000	0.964	1.02	1.05	1.08	1.08
S3	MEG	1	DCM	2.23000	0.963	1.03	1.06	1.07	1.12
S3	MEG	1	DCM	2.26000	0.900	1.02	1.09	1.10	1.11
S3	MEG	1	DCM	2.29000	0.945	1.05	1.11	1.14	1.21
S3	MEG	1	DCM	2.32000	0.941	1.06	1.11	1.14	1.16
S3	MEG	1	DCM	2.35000	1.03	1.10	1.13	1.14	1.15
S3	MEG	1	DCM	2.50000	1.09	1.16	1.20	1.24	1.25
S3	MEG	1	DCM	2.65000	1.07	1.18	1.25	1.27	1.30
S3	MEG	1	DCM	2.80000	1.18	1.29	1.34	1.38	1.40
S3	MEG	1	DCM	2.95000	1.17	1.35	1.40	1.43	1.45
S3	HEG	1	DCM	3.10000	1.24	1.36	1.46	1.53	1.54
S3	MEG	1	DCM	3.10000	1.23	1.39	1.47	1.51	1.53
S3	HEG	1	DCM	3.25000	1.26	1.44	1.57	1.64	1.65
S3	MEG	1	DCM	3.25000	1.33	1.46	1.55	1.59	1.60
S3	HEG	1	DCM	3.40000	1.34	1.47	1.57	1.64	1.66
S3	MEG	1	DCM	3.40000	1.38	1.55	1.62	1.66	1.69
S3	HEG	1	DCM	3.55000	1.39	1.58	1.68	1.75	1.78
S3	MEG	1	DCM	3.55000	1.41	1.57	1.68	1.73	1.76
S3	HEG	1	DCM	3.70000	1.44	1.59	1.71	1.82	1.84
S3	MEG	1	DCM	3.70000	1.37	1.60	1.69	1.77	1.85
S3	HEG	1	DCM	3.85000	1.46	1.62	1.76	1.83	1.87
S3	MEG	1	DCM	3.85000	1.44	1.72	1.83	1.90	1.95
S3	HEG	1	DCM	4.00000	1.44	1.65	1.85	1.92	1.96
S3	HEG	1	DCM	4.00000	1.60	1.75	1.88	1.90	1.94
S3	MEG	1	DCM	4.00000	1.43	1.65	1.81	1.89	1.92
S3	MEG	1	DCM	4.00000	1.42	1.60	1.82	1.93	1.98
S3	HEG	1	DCM	4.20000	1.58	1.75	1.86	1.93	1.96
S3	MEG	1	DCM	4.20000	1.49	1.72	1.88	1.99	2.07
S3	HEG	1	DCM	4.40000	1.60	1.83	1.93	2.03	2.06
S3	MEG	1	DCM	4.40000	1.53	1.88	2.04	2.13	2.18
S3	HEG	1	DCM	4.60000	1.76	1.95	2.08	2.21	2.21
S3	MEG	1	DCM	4.60000	1.64	1.92	2.05	2.16	2.23
S3	HEG	1	DCM	4.80000	1.72	1.95	2.17	2.24	2.25

Table 14. Low energy bandwidth size for extracting the equal number of counts, for chip S3 (part 1).

					Low Energy Limit for High Energy Limit =				
Chip	Grating	Order	Source	Energy	$0.08keV$	$0.10keV$	$0.12keV$	$0.14keV$	$0.16keV$
S3	MEG	1	DCM	4.80000	1.41	1.78	2.00	2.17	2.32
S3	HEG	1	DCM	5.00000	1.87	2.10	2.24	2.33	2.41
S3	HEG	1	DCM	5.00000	1.51	1.78	1.98	2.10	2.17
S3	MEG	-1	DCM	5.00000	1.69	2.05	2.27	2.37	2.47
S3	MEG	-1	DCM	5.00000	1.70	2.03	2.22	2.32	2.38
S3	MEG	1	DCM	5.00000	1.62	2.05	2.24	2.34	2.40
S3	MEG	1	DCM	5.00000	1.61	2.02	2.24	2.34	2.41
S3	HEG	1	DCM	5.25000	1.70	1.93	2.10	2.21	2.30
S3	MEG	-1	DCM	5.25000	1.76	2.05	2.32	2.44	2.52
S3	MEG	1	DCM	5.25000	1.71	2.09	2.31	2.44	2.50
S3	HEG	1	DCM	5.50000	1.60	1.96	2.16	2.27	2.38
S3	MEG	-1	DCM	5.50000	1.70	2.08	2.35	2.53	2.60
S3	MEG	1	DCM	5.50000	1.63	1.96	2.23	2.44	2.57
S3	HEG	1	DCM	5.75000	1.59	1.88	2.17	2.31	2.47
S3	MEG	-1	DCM	5.75000	1.75	2.11	2.38	2.54	2.71
S3	MEG	1	DCM	5.75000	1.68	2.09	2.38	2.61	2.74
S3	HEG	1	DCM	6.00000	1.67	2.07	2.35	2.54	2.66
S3	MEG	-1	DCM	6.00000	2.04	2.42	2.69	2.79	2.85
S3	MEG	1	DCM	6.00000	1.74	2.18	2.45	2.68	2.75
S3	HEG	1	DCM	6.25000	1.61	2.05	2.31	2.49	2.68
S3	MEG	-1	DCM	6.25000	1.88	2.49	2.74	2.91	3.02
S3	MEG	1	DCM	6.25000	1.74	2.15	2.61	2.83	2.93
S3	HEG	1	Fe	6.40380	1.90	2.21	2.50	2.73	2.84
S3	MEG	-1	Fe	6.40380	2.33	2.66	2.86	3.00	3.08
S3	MEG	1	Fe	6.40380	2.19	2.51	2.78	3.00	3.12
S3	HEG	1	DCM	6.50000	1.71	2.22	2.54	2.71	2.86
S3	MEG	-1	DCM	6.50000	2.18	2.58	2.83	3.04	3.14
S3	MEG	1	DCM	6.50000	1.82	2.15	2.64	2.79	2.90
S3	HEG	1	DCM	6.75000	1.77	2.14	2.52	2.83	2.94
S3	MEG	-1	DCM	6.75000	2.14	2.48	2.72	2.91	3.11
S3	MEG	1	DCM	6.75000	1.71	2.47	2.63	2.75	2.83
S3	HEG	1	DCM	7.00000	1.92	2.42	2.82	3.06	3.20
S3	MEG	-1	DCM	7.00000	1.90	2.72	3.05	3.29	3.51
S3	MEG	1	DCM	7.00000	1.73	2.25	2.88	3.22	3.36
S3	HEG	1	DCM	7.20000	1.56	2.05	2.38	2.67	2.86
S3	MEG	-1	DCM	7.20000	2.39	2.81	3.07	3.39	3.53
S3	MEG	1	DCM	7.20000	2.00	2.35	2.81	3.07	3.26
S3	HEG	1	DCM	7.70000	1.85	2.26	2.57	2.91	3.15
S3	MEG	-1	DCM	7.70000	2.38	3.13	3.13	3.46	3.70
S3	MEG	1	DCM	7.70000	2.30	2.80	2.96	3.19	3.29
S3	HEG	1	Cu	8.04780	1.92	2.25	2.61	2.80	3.03
S3	HEG	1	DCM	8.20000	2.00	2.45	2.95	3.36	3.60
S3	MEG	-1	DCM	8.20000	2.72	2.72	2.75	3.08	3.08
S3	MEG	1	DCM	8.20000	1.61	2.28	2.48	3.03	3.72
S3	HEG	-1	DCM	8.70000	1.80	2.60	2.83	3.12	3.53
S3	HEG	1	DCM	8.70000	1.68	2.37	2.91	3.43	3.69
S3	MEG	-1	DCM	8.70000	1.78	1.78	2.17	3.70	3.70
S3	MEG	1	DCM	8.70000	2.50	2.26	3.16	2.50	2.50

Table 15. Low energy bandwidth size for extracting the equal number of counts, for chip S3 (part 2).

					Low Energy Limit for High Energy Limit =				
Chip	Grating	Order	Source	Energy	$0.08keV$	$0.10keV$	$0.12keV$	$0.14keV$	$0.16keV$
S4	MEG	1	DCM	0.950000	0.512	0.512	0.512	0.512	0.512
S4	MEG	1	DCM	1.00000	0.517	0.517	0.517	0.517	0.517
S4	MEG	1	DCM	1.05000	0.545	0.545	0.545	0.540	0.540
S4	MEG	1	DCM	1.10000	0.563	0.563	0.563	0.567	0.567
S4	MEG	1	DCM	1.15000	0.582	0.587	0.596	0.596	0.596
S4	MEG	1	DCM	1.20000	0.652	0.654	0.654	0.771	0.771
S4	MEG	1	DCM	1.25000	0.627	0.631	0.631	0.631	0.643
S4	HEG	1	DCM	1.30000	0.653	0.653	0.653	0.653	0.653
S4	HEG	1	DCM	1.35000	0.682	0.702	0.702	0.702	0.702
S4	HEG	1	DCM	1.40000	0.693	0.706	0.708	0.708	0.708
S4	HEG	1	DCM	1.40000	0.698	0.698	0.701	0.701	0.701
S4	HEG	1	DCM	1.43000	0.702	0.721	0.721	0.721	0.727
S4	HEG	1	DCM	1.46000	0.807	0.807	0.807	0.807	0.807
S4	HEG	1	Al	1.48670	0.731	0.745	0.745	0.745	0.749
S4	HEG	1	DCM	1.49000	0.736	0.736	0.736	0.744	0.744
S4	HEG	1	DCM	1.52000	0.758	0.758	0.758	0.758	0.758
S4	HEG	1	DCM	1.55000	0.777	0.778	0.778	0.778	0.778
S4	HEG	1	DCM	1.58000	0.775	0.822	0.822	0.822	0.822
S4	HEG	1	DCM	1.61000	0.790	0.808	0.812	0.812	0.812
S4	HEG	1	DCM	1.64000	0.832	0.833	0.833	0.833	0.833
S4	HEG	1	DCM	1.67000	0.838	0.849	0.851	0.851	0.851
S4	HEG	1	DCM	1.70000	0.851	0.859	0.890	0.902	0.902
S4	HEG	1	DCM	1.86000	0.949	1.00	1.00	1.00	1.00
S4	HEG	1	DCM	1.88000	0.898	0.915	0.927	0.927	0.933
S4	HEG	1	DCM	1.90000	0.893	0.951	0.978	0.978	1.03
S4	HEG	1	DCM	1.92000	0.967	0.994	0.994	0.994	1.03
S4	HEG	1	DCM	1.94000	0.964	0.967	0.967	0.967	0.967
S4	HEG	1	DCM	1.96000	0.976	0.986	1.04	1.04	1.04
S4	HEG	1	DCM	1.98000	0.969	0.969	0.969	0.970	0.970
S4	HEG	1	DCM	2.00000	0.968	0.977	0.990	1.00	1.00
S4	HEG	1	DCM	2.05000	1.01	1.02	1.02	1.02	1.02
S4	HEG	1	DCM	2.08000	1.04	1.21	1.21	1.21	1.21
S4	HEG	1	DCM	2.11000	1.01	1.13	1.13	1.13	1.13
S4	HEG	1	DCM	2.14000	1.05	1.17	1.17	1.17	1.17
S4	HEG	1	DCM	2.17000	1.01	1.01	1.01	1.01	1.01
S4	HEG	1	DCM	2.20000	1.08	1.08	1.10	1.10	1.10
S4	HEG	1	DCM	2.23000	1.09	1.09	1.09	1.09	1.09
S4	HEG	1	DCM	2.26000	1.15	1.15	1.15	1.15	1.15
S4	HEG	1	DCM	2.29000	1.11	1.12	1.12	1.12	1.12
S4	HEG	1	DCM	2.32000	1.07	1.07	1.07	1.07	1.07
S4	HEG	1	DCM	2.35000	1.15	1.18	1.18	1.18	1.18
S4	HEG	1	DCM	2.50000	1.17	1.17	1.17	1.17	1.17
S4	HEG	1	DCM	2.65000	1.25	1.27	1.34	1.34	1.34

Table 16. Low energy bandwidth size for extracting the equal number of counts, for chip S4.

					Low Energy Limit for High Energy Limit =				
Chip	Grating	Order	Source	Energy	$0.08keV$	$0.10keV$	$0.12keV$	$0.14keV$	$0.16keV$
S4/S5	HEG	1	DCM	1.20000	0.572	0.572	0.572	0.572	0.600
S4/S5	HEG	1	DCM	1.25000	0.694	0.694	0.694	0.694	0.694

Table 17. Low energy bandwidth size for extracting the equal number of counts, for lines spanning the gap between chips S4 and S5.

					Low Energy Limit for High Energy Limit =				
Chip	Grating	Order	Source	Energy	$0.08keV$	$0.10keV$	$0.12keV$	$0.14keV$	$0.16keV$
S5	MEG	1	O	0.524900	0.260	0.260	0.260	0.260	0.260
S5	HEG	1	DCM	0.950000	0.449	0.449	0.449	0.449	0.449
S5	HEG	1	DCM	1.00000	0.445	0.445	0.445	0.445	0.445
S5	HEG	1	DCM	1.05000	0.654	0.654	0.654	0.654	0.654
S5	HEG	1	DCM	1.10000	0.554	0.554	0.554	0.554	0.554
S5	HEG	1	DCM	1.15000	0.582	0.585	0.718	0.718	0.718

Table 18. Low energy bandwidth size for extracting the equal number of counts, for chip S5.

REFERENCES

1. K. Allen, P. P. Plucinsky, B. R. McNamara, R. J. Edgar, N. S. Schulz, "A Study of the AXAF Effective Area with the ACIS Detector", `http://asc.harvard.edu/cal/Links/Acis/acis/Cal_prods/effarea/Aeff.ppp.ps`, (February 14, 1999).
2. M. Bautz, J. Nousek, G. Garmire and the ACIS instrument team, "Science Instrument Calibration Report for the AXAF CCD Imaging Spectrometer (ACIS), Version 2.20", (1999).
3. K. J. Glotfelty, "ACIS Grading Scheme Recommendation", `http://hea-www.harvard.edu/acis/xrcf/grade.html`, (1997).
4. J. H. Kastner, CSC implementation of ACIS event grading schemes: a Memorandum to CXC ACIS, ACIS IPI, and MSFC Science Teams (V 1.1), `http://space.mit.edu/ASC/docs/grades.ps`, (April 2, 1999).
5. Science Instrument Operations Handbook, ACIS-PSU-SOP-01, Version 2.65, J. Nousek, PSU, `http://acis.mit.edu/sop01.v265/`, (November 20, 1997).
6. N. S. Schulz, D. Dewey, and H. L. Marshall, "Absolute Effective Areas of the HETGS", `http://space.mit.edu/HETG/papers/spie98_effarea.ps`, (June 1998).
7. N. S. Schulz, S. C. Taylor, D. Dewey, and H. L. Marshall, "Absolute Effective Areas of the HETGS", (1999).